Effects of low-density lipoprotein receptor-related protein 4 and apolipoprotein E isoforms on bone metabolism *in vivo*

Dissertation

Zur Erlangung des Grades

Doktor der Naturwissenschaften

Am Fachbereich Biologie

Der Johannes Gutenberg-Universität, Mainz

Marco Dieckmann

Geboren am 3. Februar 1980 in Bremen

Mainz, November, 2010

Dekan:

1. Berichterstatter:
2. Berichterstatter:

Tag der mündlichen Prüfung: 3. Dezember 2010

Dedication

This thesis is dedicated to my mother and my wife,

who have supported me unconditionally

ACKNOWLEDGMENTS

I would first like to acknowledge my mentor and for giving me the opportunity to work, learn, and grow in their laboratories. Thank you for all your supervision, support, and encouragement during the past years.

Thanks to all co-workers in the lab. , thanks for introducing me into this lab group. Your advice and our scientific discussions were very helpful to me. , , and , it was always fun with you guys sharing the same lab - stay as you are. , , and , I enjoyed our time in lab and look forward to seeing you guys soon. , thank you for all your help and your contribution to my projects – I appreciate it.

Thanks for all co-workers in the lab. , thank you for introducing me into the and your scientific advice. , thanks for all your help in and outside the lab. We had a great time and started some great projects. I look forward to finishing them together with you. , thank you for the opportunity to finish the LRP4 ECD together with you. , thank you for being my student and your great contribution to my projects. , , , and , you are great co-workers. Thank you for your support and the fruitful scientific discussions. , , , and , thank you for the indispensable technical support and keeping me motivated.

Special thanks to my collaborator , who is an outstanding scientist. My thesis is based on projects which are a direct result of this collaboration. I hope that we will be working together for a long time.

I am grateful for the funding of the . This scholarship gave me the opportunity to continue my projects in one of the leading laboratories on LRP research and to experience living and working a foreign country.

After all these scientific acknowledgments, I want to thank my mom, who supported and encouraged me throughout my whole study – I hope this title gives something back to you.

I thank my family and my friends for their help and their backup even though 9000 kilometers separated us – I will always keep that in mind.

In the end and most importantly, I would like to thank my wife, , for accompanying me on this journey. Your love and your selfless support made everything so easy - I love you.

ABSTRACT

LRP4, a novel receptor for Dickkopf1 and sclerostin, is expressed by osteoblasts and regulates bone growth and turnover *in vivo*.

LRP4, member of the LDLR family, is a multifunctional membrane-bound receptor that is expressed in various tissues. The expression of LRP4 by osteoblasts, its novel interaction with Wnt-signaling inhibitors Dkk1 and SOST, and the lower levels of activated β-catenin in different bone locations described here, adds another player to the long list of established factors that modulate canonical Wnt-signaling in bone. By demonstrating that in addition to Wise, LRP4 is able to interact with two additional important modulators of Wnt- and BMP-signaling, our perspective of the complexity of the integration of BMP and Wnt-signaling pathways on the osteoblast surface has expanded further. Nevertheless the recently described association of both the SOST and LRP4 genes with BMD in humans, together with our findings suggest that LRP4 plays a physiologically important role in the skeletal development and bone metabolism not only in rodents, but in humans as well. The efficiency with which LRP4 binds both SOST and Dkk1, presumably at the osteoblastic surface, LRP4 may act as a sink and competes with LRP5/6 for the binding of these Wnt antagonists, which then are no longer available for suppression of the signal through the LRP5/6 axis.

Impact of apolipoprotein E gene polymorphisms ε2, ε3, and ε4 on bone metabolism

ApoE, a 299 amino acid glycoprotein, is a crucial regulator in the uptake of triglyceride, phospholipids, cholesteryl esters, and cholesterol into cells. ApoE has been linked to osteoporosis, and such a role is further strengthened by the present of a high bone mass phenotype in ApoE null mice. Until recently, the effects of respective ApoE isoforms E2, E3, and E4, and their impact on bone metabolism, have been unclear. Here we report that respective human ApoE knockin mice display diverse effects on bone metabolism. ApoE2 mice show decreased trabecular bone volume per total volume in femoral bone and lumbar spine in comparison to ApoE3 and E4 animals. In this context, urinary bone resorption marker DPD is increased in these animals, which is accompanied by a low ratio of osteoclastogenesis markers OPG/RANKL. Interestingly, serum bone formation markers ALP and OCN are diminished in ApoE4 mice. In contrast to this finding, ApoE2 mice show the lowest bone formation of all groups *in vivo*. These findings cannot be explained by the low receptor-affinity of ApoE2 and subsequent decreased uptake of triglyceride-rich lipoproteins by osteoblasts, resulting in elevated levels of undercarboxylated osteocalcin. Thus, other crucial pathways relevant for bone metabolism, e. g. Wnt/β-catenin-signaling pathways, must be, compared to the ApoE3/4 isoforms, more affected by the ApoE2 isoform.

Index

ABBREVIATIONS

AD	Alzheimer´s Disease
ADAM	Disintegrin and metalloproteinase domain-containing protein
AER	Apical ectodermal ridge
ALP	Alkaline Phosphatase
APC	Adenomatous polyposis coli
Apo	Apolipoprotein
Apoer2	Apolipoprotein receptor 2
ATF4	Activating transcription factor 4
BMC	Bone mineral content
BMD	Bone mineral density
BMP	Bone morphogenic protein
CK1	Casein kinase 1
CLS	Cenani-Lenz Syndrome
CM	Chylomicron
CR	Chylomicron remnant
Dkk1	Dickkopf1
DPD	Deoxypyridinoline
DSH	Dishevelled
ECD	Extracellular domain
ECM	Extracellular matrix
EC-Stop	Extracellular-stop
EGF	Epidermal growth factor
EtOH	Ethanol
FGF	Fibroblast growth factor
FH	Familial hypercholesterolemia

Fz	Frizzled receptors
GSK3β	Glycogen synthase kinase 3β
HEK	Human embryonic kidney
HBM	High bone mass
HDL	high-density lipoprotein
IACUC	Institutional Committee for Use and Care of Laboratory Animals of the University of Texas Southwestern Medical Center at Dallas
ICD	intracellular domain
LDL	Low-density lipoprotein
LDLR	Low-density lipoprotein receptor
LEF	Lymphoid enhancer factor
LOAD	Late-onset Alzheimer´s Disease
LRP1	Low-density lipoprotein receptor related protein 1
LRP1B	Low-density lipoprotein receptor related protein 1B
LRP2	Low-density lipoprotein receptor related protein 2
LRP4	Low-density lipoprotein receptor related protein 4
LRP8	Low-density lipoprotein receptor related protein 8
M-CSF	Macrophage colony-stimulating factor 1
MEGF7	Multiple epidermal growth factor like domains 7
MUSK	Muscle-specific tyrosine kinase
NCBI	National Center for Biotechnology Information
NMJ	Neuromuscular junction
OCN	Osteocalcin
OPG	Osteoprotegorin
OPS	Osteoporosis-Pseudoglioma Syndrome

PBS	Phosphate buffered saline
PCR	Polymerase chain reaction
PFA	Paraformaldehyde
RANK	Receptor activator for nuclear factor κ B
RANKL	Receptor activator for nuclear factor κ B ligand
RAP	Receptor-associated protein
RIP	Regulated intramembraneous processing
RNA	Ribonucleic acid
ROI	Region of interest
RS2	R-spondin2
RT	Room temperature
RT-PCR	Real-time PCR
Runx2	Runt-related transcription factor 2
Shh	Sonic hedgehog
SNP	Single nucleotide polymorphism
SOST	Sclerostin
TCF	T-cell factor
TNF	Tumor necrosis factor
UTSW	University of Texas Southwestern
VLDL	Very low-density lipoprotein
VLDLR	Very low-density lipoprotein receptor
VPS	Vacuolar protein sorting

List of Figures

1. Introduction

1.1 Part 1 – LRP4 in bone mabolism

1.1.1 The low-density lipoprotein receptor gene family

The low-density lipoprotein (LDL) receptor gene family is an evolutionarily ancient and multifunctional protein family whose members are expressed on the surface of many cell types (Herz et al. 2002). Over 30 years ago the namesake of the LDL receptor gene family, the low-density lipoprotein receptor (LDLR), was originally identified as the gene that is defective in autosomal codominant form of familial hyper-cholesterolemia (Goldstein et al. 2001). Until now, the core of the LDL receptor gene family consists of LDLR, the very-low density lipoprotein receptor (VLDLR), the apolipoprotein E receptor 2 (Apoer2 or LRP8), low-density lipoprotein receptor related protein 4 (LRP4; also known as multiple epidermal growth factor like domains 7 (MEGF7)), the low-density lipoprotein receptor related protein 1 (LRP1), and the structurally and in size most similar LRP1B and LRP2 (Megalin) (May et al. 2003) (Figure 1). They all share the same motifs in the same repeating arrangement, where ligand binding type cysteine-rich repeats are always followed by a YWTD-motif containing a ß-propeller domain that is flanked by epidermal growth factor (EGF) like cysteine-rich repeats. These receptors are anchored in the plasma membrane by a single membrane-spanning segment. A short cytoplasmic tail contains one or more NPxY motifs, which represent the major binding sites for adaptor proteins (Gotthardt et al. 2000). LRP5, LRP6, and SorLa represent a more distantly related subgroup which share some, but not all, of the structural hallmarks that define the core of the family. In addition, they may also contain structural and functional domains, which are not present in the core members (May et al. 2005) (Figure 1)

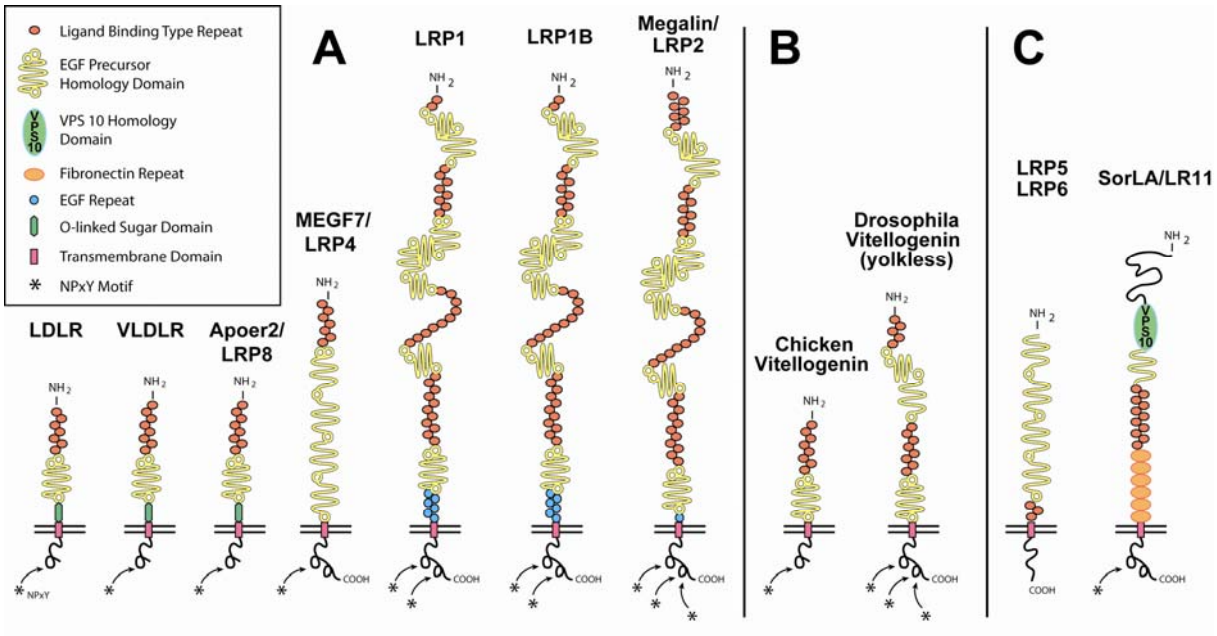

Figure 01 - The LDL receptor gene family

(**A**) The core low-density lipoprotein (LDL) receptor gene family as it exists in mammalian species. These family members are characterized by one or more ligand binding domains, epidermal growth factor (EGF), homology domains consisting of EGF repeats and YWTD propeller (β-propeller) domains, a single transmembrane domain and a cytoplasmic tail containing at least one NPxY motif. The latter represents both the endocytosis signal as well as a binding site for adaptor proteins linking the receptor to intracellular signaling pathways. Furthermore, LDLR, VLDLR, and Apoer2 carry an O-linked sugar domain. (**B**) Equivalent receptors that are structurally and functionally distinct family members in non-mammalian species. (**C**) A subgroup of functionally important, but more distantly related family members that share some, but not all, of the structural requirements of the 'core members'. In addition, they could also contain domains, e.g. vacuolar protein sorting (VPS) domain, which are not present in the core family (from Herz et al. 2008).

Originally, these cell surface proteins were thought to merely mediate the traffic of lipids and nutrients between cells and in some cases, by functioning as scavenger receptors, and remove other kinds of macromolecules, such as proteases and protease inhibitors from the extracellular space and the cell surface. This picture has greatly expanded over the last decade. By physically interacting and coevolving with fundamental signaling pathways, lipoprotein receptors are deeply embedded in the machinery by which cells communicate with each other (Herz et al. 2006). This rapidly expanding role of the LDL receptor gene family implies various functions for

the different members. The founding member of the LDL receptor gene family plays the indispensible role of regulating cholesterol homeostasis by binding to cholesterol-rich LDL particles and subsequent endocytosis of the receptor-ligand complex (Brown and Goldstein, 1979). Mutations in the LDLR gene account for familial hypercholesterolemia (FH) leading to increased plasma cholesterol concentrations causing premature cardiovascular disease (Hobbs et al. 1990). VLDLR and Apoer2 are key receptors in the signaling pathway of reelin and the proper lamination of the cortex and Purkinje cell localization in the cerebellum during development (Trommsdorff et al. 1999). LRP4 is a crucial regulator in kidney (Li et al 2010; Karner et al. 2010) and tooth development (Johnson et al. 2005) and an essential co-receptor for agrin in the formation of neuromuscular junctions (Weatherbee et al. 2006). LRP1 is one of the largest – together with LRP1B and LRP2 – and most versatile receptors of the LDL receptor gene family. This receptor is, among others, involved in the endocytosis of a broad range of ligands and acts as a receptor for chylomicron remnants as well as lipases (Beisiegel et al. 1991). Moreover, LRP1 is a negative modulator of PDGF-signaling and suppression of atherosclerosis (Boucher et al. 2003, Takayama et al. 2005, Zhou et al. 2009). It regulates the production (Li et al. 2000; Cam et al. 2005) and translocation of Aβ (Shibata et al. 2000; Deane et al. 2004), suggesting a possible involvement in the pathogenesis of Alzheimer´s Disease (AD). LRP1B is the closest relative to LRP1 and the fourth most frequently mutated gene in non-small cell lung carcinomas (Liu et al. 2000; Ding et al. 2008). Follow up studies further discovered mutations or deletions of LRP1B in other cancer types (Langbein et al. 2002; Sonoda et al. 2004; Roversi et al. 2006; Nakagawa et al. 2006; Rahmatpanah et al. 2006; Taylor et al. 2007) indicating a crucial role in cellular growth regulation and cancer development. LRP2 also binds numerous extracellular ligands including various vitamins and

nutrients (Nykjaer et al. 1999; Willnow and Nykjaer et al. 2002), sonic hedgehog (Shh), and bone morphogenetic protein (BMP) 4 (Spoelgen et al. 2005). LRP5 and LRP6 are essential co-receptors for the Wnt-signaling pathway which controls multiple developmental processes (Pinson et al. 2000; Tamai et al. 2000).

1.1.2 LRP4, a member of the LDL receptor gene family

LRP4, also known as MEGF7, was identified in 1998 during a motif trap screening of gene encoding proteins with multiple epidermal growth factor (EGF) like motifs in human brain coding DNA libraries (Nakayama et al. 1998). This cell surface receptor belongs to the core LDL receptor gene family and shares all its structural hallmarks (May et al. 2003). LRP4 is unique in its size, which lies between the small members of the family (LDLR, VLDLR, and Apoer2) and the large receptors represented by LRP1, LRP1B, and LRP2. It also possess an NPxY motif in its cytoplasmic domain, a tetraamino acid sequence that has been shown to mediate the coupling of these receptors to both the endocytic machinery (Chen et al. 1990) and to a wide range of intracellular signaling cascades (Nykjaer et al. 2002).

Interestingly, *in vitro* evidence indicates a metalloproteinase-mediated cleavage of the extracellular domain (ECD) of LRP4 and regulated intramembraneous processing (RIP) by γ-secretase (Dietrich et al. 2010). Both cleavage steps have important physiological functions in other LDL gene family members including signal modulation and transcriptional inhibition. However, these cleavage events will have to be verified and evaluated *in vivo* (Dietrich et al. 2010).

1.1.3 The physiological function of LRP4

The physiological function of LRP4 had been unclear until a few years ago. To gain insight into its biological role Johnson and colleagues disrupted the LRP4 gene via homologous recombination by introducing a stop codon just upstream the transmembrane segment (Figure 2).

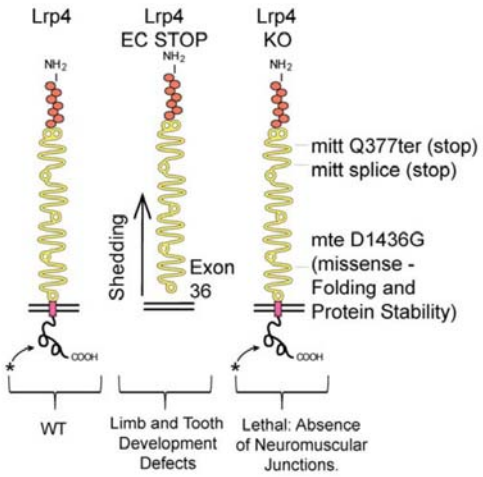

Figure 02 - Illustration of wild-type low-density lipoprotein receptor-related protein 4 (LRP4), the LRP4 mutant extracellular stop (EC-Stop), and known mutations of the low-density lipoprotein and their respective phenotypes.

The known mutations in murine models for LRP4 are shown. The presence of the extracellular domain (ECD) rescues the lethality caused by the complete functional null mutation (from Dietrich et al. 2010).

Homozygous LRP4 mutant mice are growth retarded (Figure 3B), with fully penetrant polysyndactyly in their fore and hind limbs (Figure 3A), and partially penetrant abnormalities of tooth development (Figure 3C). The reason for this developmental abnormality is apparent as early as embryonic day 9.5 when the apical ectodermal ridge (AER), the principal site of LRP4 expression at the distal edge of the embryonic limb bud, forms abnormally in the absence of functional LRP4 (Johnson et al. 2005).

Interestingly, positional cloning of two novel independent recessive mutations at the LRP4 locus in the mouse results in the same phenotype of polysyndactyly as LRP4 ECD (Simon-Chazottes et al. 2006). LRP4 loss-of-function have also spontaneously and independently arisen in several viable cattle strains (Duchesne et al. 2006; Drogemüller et al. 2007).

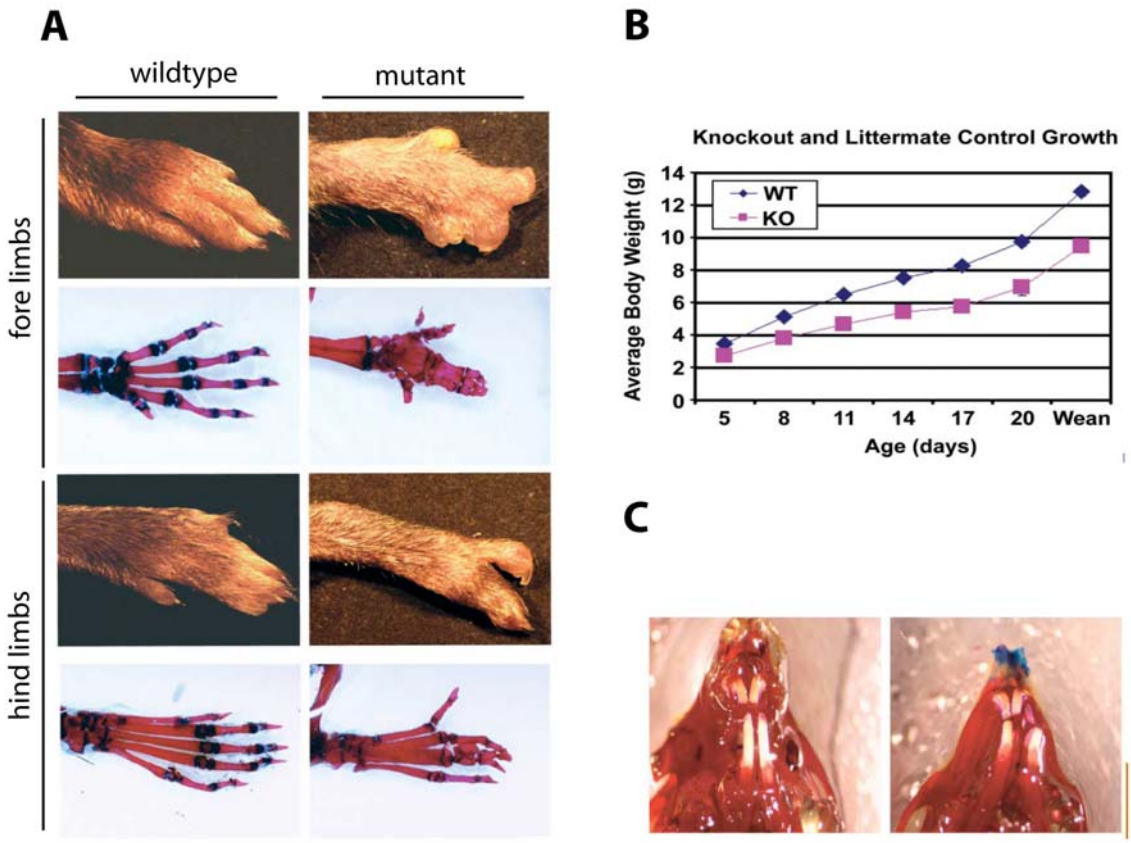

Figure 03 - known phenotypes of mutations in LRP4 and LRP4 ECD in mice.
(**A**) Polysyndactyly, a phenotype that is characterized by the fusion and duplication of digits at both the fore and the hind limbs, in adult low-density lipoprotein receptor-related protein (LRP4) mutant mice. (**B**) Growth curves of wildtype and heterozygous (filled diamonds) and LRP4 extracellular domain (ECD) (filled squares) pups from P5 until weaning (P23). (**C**) Abnormal tooth development is apparent in some LRP4 ECD mice (from Johnson et al. 2005).

In contrast to the aforementioned LRP4 mutants, Weatherbee and colleagues identified two LRP4 mutants that cause perinatal lethality with striking and similar defects in limb development, suggesting that those mutations that allow postnatal development are functional hypomorphs (Weatherbee et al. 2006). One of the

striking phenotypes caused by a complete lack of the LRP4 is paralysis at birth, due to an early block in the development of a specialized synapse, the neuromuscular junction (NMJ) (Weatherbee et al. 2006). LRP4 functions as an obligate coreceptor for the muscle-specific tyrosine kinase (MUSK) and is required for the activation of MUSK by the signaling protein Agrin (Kim et al. 2008; Zhang et al. 2008). This mechanism combines the absolute requirement of LRP4 as a unique receptor and the ability to indirectly control of this primary signaling mechanism.

1.1.4 Role of LRP4 in the Wnt-signaling pathway

The Wnt-signaling pathway plays an important role in embryonic development (Logan et al. 2004). Abnormal Wnt-signaling has been associated with human diseases ranging from cancer to degenerative diseases (Clevers et al. 2006). The Wnt family consists of 19 secreted cystein-rich glycoproteins which, among other pathways, activate the canonical Wnt-signaling pathway by binding a complex consisting of frizzled receptors (Fz) and the co-receptors LRP5/6. This pathway mediates important biological processes including cell proliferation and survival, cell fate, and embryogenesis (Moon et al. 2004). In the absence of Wnt ligands in the canonical Wnt-signaling pathway, β-catenin is recruited into the "destruction complex" that comprises of the adenomatous polyposis coli (APC) and Axin2, which facilitate the phosphorylation of β-catenin by casein kinase 1 (CK1) and then glycogen synthase kinase 3β (GSK3β). This phosphorylation event leads to the ubiquitylation and proteasomal degradation of β-catenin (Moon et al. 2004) (Figure 4A). If the local concentration of Wnt proteins exceeds the buffering capacity of inhibitors, Wnt ligands bind to Fz and LRP5/6 in a ternary complex at the cell surface leading to the activation of the phosphoprotein dishevelled (DSH). The activation and membrane recruitment of DSH recruits Axin2 and the destruction complex to the

plasma membrane, where Axin2 directly binds to the cytoplasmic tail of LRP5/6. Therefore, the “destruction complex” as well as GSK3β are inhibited and β-catenin accumulates within the cell (He et al. 2004). Subsequently, β-catenin translocates to the nucleus, where it interacts with DNA-bound lymphoid enhancer factor (LEF) and T-cell factor (TCF) to activate the transcription of target genes (Clevers et al. 1997) (Figure 4B).

Digit formation results from complex and coordinated interactions between several signaling molecules, e.g. fibroblast growth factors (FGF), bone morphogenetic proteins (BMP), Wnts, and sonic hedgehog (Shh) (Capdevila et al. 2001). In LRP4 ECD mice several of the aforementioned signaling proteins (FGF8, Shh, BMP2, BMP4, and Wnt7a) as well as the Wnt- and BMP-responsive transcription factors Lmx1b and Msx1 are abnormally expressed. In addition, LRP4 inhibits the Wnt-induced activation of the luciferase reporter in a Wnt activity assay, suggesting that LRP4 can antagonize the LRP5/6- mediated activation of this signaling pathway (Johnson et al. 2005) (Figure 4C). These findings suggest a role for LRP4 as a modulator of the signaling pathways that control limb development in the embryo.

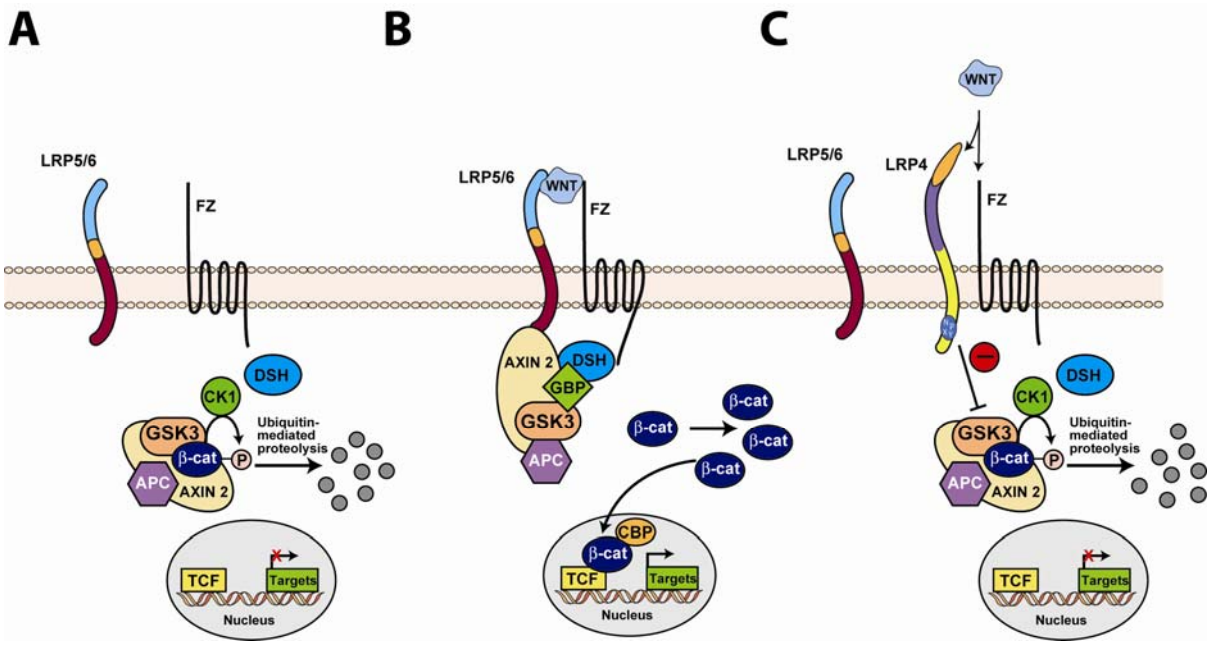

Figure 04 - Involvement of the LRP4 in Wnt-signaling.

(**A**) In the absence of Wnt ligands in the canonical Wnt-signaling pathway, β-catenin is recruited into the "destruction complex" that comprises of the adenomatous polyposis coli (APC) and Axin2, which facilitate the phosphorylation of β-catenin by casein kinase 1 (CK1) and then glycogen synthase kinase 3β (GSK3β). This phosphorylation event leads to the ubiquitylation and proteasomal degradation of β-catenin. (**B**) If Wnt proteins bind to Fz and LRP5/6 in a ternary complex at the cell surface leading to the activation of the phosphoprotein dishevelled (DSH). The activation and membrane recruitment of DSH recruits Axin2 and the destruction complex to the plasma membrane, where Axin2 directly binds to the cytoplasmic tail of LRP5/6. Therefore, the "destruction complex" as well as GSK3β are inhibited and β-catenin accumulates within the cell. Subsequently, β-catenin translocates to the nucleus, where it interacts with DNA-bound lymphoid enhancer factor (LEF) and T-cell factor (TCF) to activate the transcription of target genes. (**C**) The suggested role of LRP4 as an antagonist of canonical Wnt-signaling pathway is thought to be mediated in part by a displacement of the homologous LRP5/6 proteins in the co-receptor complex formed by Fz with LRP5/6, which is required to bind Wnt proteins and to transduce the Wnt signal to downstream elements of the canonical cascade.

In tooth morphogenesis, LRP4 modulates and integrates BMP and canonical Wnt-signaling by binding the secreted BMP antagonist protein, Wise. This interaction results in the modulation of Wnt-signaling in the epithelial cells. In this context, Wise, secreted by mesenchyme cells, acts as an extracellular molecule linking the BMP and Wnt-signaling pathways via LRP4 (Ohazama et al. 2008).

In a homozygosity-mapping approach, Li and colleagues mapped the locus of the Cenani-Lenz syndrome (CLS) – an autosomal-recessive congenital disorder affecting distal limb development – to chromosome 11p11.2q13.1 and identified mutations in the LRP4 gene in 12 CLS families. In addition, to the well-described distal limb malformation, over 50% of CLS families present renal agenesis and/or hypoplasia (Li et al. 2010). Spatial and temporal activation of canonical Wnt/β-catenin-signaling is an essential developmental process during organogenesis and tissue regeneration (Clevers et al. 2006). LRP4 is important for control and modification of Wnt-signaling by its suggested antagonistic effect on LRP6-mediated activation of Wnt-signaling. This antagonistic function is completely lost in four out of five LRP4 mutants in a dual luciferase reporter assay (Li et al. 2010). Intriguingly, LRP4 null mice show a delay in ureteric bud (UB) formation that results in unilateral or bilateral kidney agenesis. A comparable phenotype could be observed in mice overexpressing β-catenin (Karner et al. 2010). These findings clearly show that LRP4 is a critical regulator for kidney development in mice and humans.

1.1.5 Role of LRP4 in bone metabolism

Although much progress has been made in the molecular understanding of bone metabolism in recent years, no therapy is yet available to cure osteoporosis (Deal et al. 2009). Many current approaches to identify potential therapeutic targets are focused on the Wnt/β-catenin-signaling pathway, which is of fundamental importance for osteogenesis (Baron et al. 2007). The structural organization of the extracellular domain of LRP4 closely resembles that of LRP5/6, two members of a subgroup of LRPs that function as co-receptors in the Wnt-signaling cascade (Tamai et al. 2000). The suggested role of LRP4 as an antagonist of canonical Wnt-signaling pathway is thought to be mediated in part by a displacement of the

homologous LRP5/6 proteins in the co-receptor complex formed by Fz with LRP5/6, which is required to bind Wnt-proteins and to transduce the Wnt-signal to downstream elements of the canonical cascade.

Bone mineral density (BMD) is a heritable complex trait used in the clinical diagnosis of osteoporosis and the assessment of fracture risk. In collaborative large-scale meta-analysis of genome-wide association studies at least 20 loci associated with lumbar spine and femoral neck BMD, e.g. LRP4, LRP5, β-catenin, osteoprotegorin (OPG), receptor activator for nuclear factor κ B ligand (RANKL), Sclerostin (SOST) etc., were identified and/or confirmed, highlighting the complex genetic architecture that underlies the variation in BMD (Rivadeneira et al. 2009; Richards et al. 2009). These findings highlight molecules within novel and known biological pathways that influence BMD variation, particularly the Wnt- and NF-κB-signaling pathway (Rivadeneira et al. 2009).

1.2 Part 2 – ApoE in bone metabolism

1.2.1 The apolipoprotein family

Apolipoproteins are components of plasma lipoproteins that can be separated into four major density classes: chylomicrons, very low-density lipoproteins (VLDL, low-density lipoproteins (LDL), and high-density lipoproteins (HDL). The major function of apolipoproteins is lipid transport in the intravascular and extravascular compartments (Li et al. 1988). Apolipoproteins are amphiphathic in nature, in that they have both hydrophobic and hydrophilic regions, and can therefore interact both with the lipids of the lipoprotein and the aqueous environment. Because of the nature of these amphipathic regions, apolipoproteins act as detergents, and have a major role in determining and stabilizing the size and structure of the lipoprotein particle (Segrest et al. 1994). Plasma apolipoproteins can be grouped into two classes, the nonexchangeable apolipoproteins (apolipoprotein (Apo) B-100 and ApoB-48), and the exchangeable apolipoproteins (ApoA, ApoC, and ApoE) (Segrest et al. 1992).

1.2.2 ApoE, a member of the apolipoprotein family

ApoE is a glycoprotein of 299 amino acids with a molecular weight of 35kDa. In the periphery, ApoE facilitates the transport of triglyceride, phospholipids, cholesteryl-esters, and cholesterol into cells, by mediating the binding, internalization, and catabolism of lipoprotein particles (Eichner et al. 2002). Plasma ApoE originates predominately from the liver (Bellosta et al. 1995) but is also expressed in a wide variety of other tissues including brain, spleen, lung, adrenal gland, ovary, and kidney (Mahley et al. 1988). Isoelectric focusing-based studies have revealed three main isoforms of ApoE in humans (Mahley et al. 1988) with single amino-acid substitutions at position 112 and 158 (Martins et al. 1995). ApoE3 (ε3) contains

cysteine and arginine, respectively, whereas ApoE2 (ε2) has two cysteines and ApoE4 (ε4) has two arginines at these positions (Weisgraber et al. 1981). A “domain interaction” occurs between Arg_{61}. A “domain interaction” has been identified between Glu_{255} in the C-terminal domain of ApoE4 and Arg_{61} in the N-terminal domain, and this interaction is enhanced by the presence of Arg_{112} in ApoE4. Although mouse ApoE is similar to human ApoE4, in that it contains Arg at position 112, murine ApoE lacks Arg_{61}. Thus, the domain interaction between Arg_{61} and Glu_{255} is prevented so that mouse ApoE behaves functionally like human ApoE3 (Vance et al. 2010) (Figure 5).

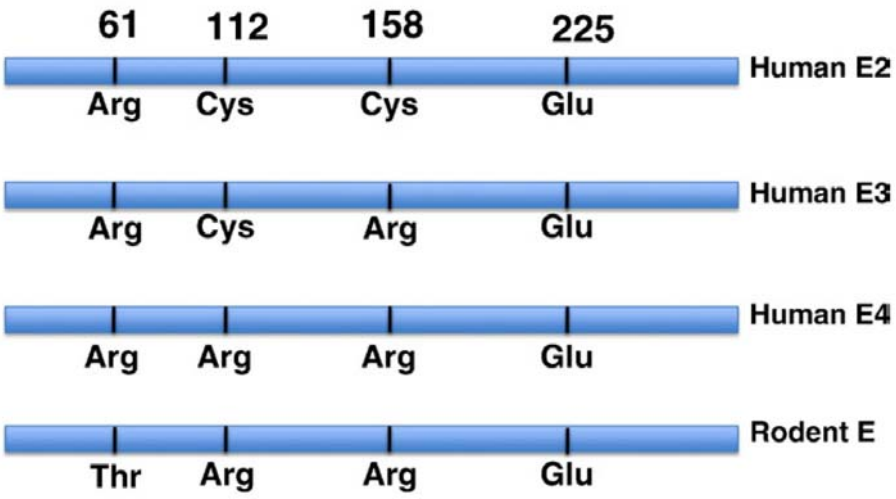

Figure 05 - Schematic representation of ApoE isoforms in humans.

Humans express 3 major isoforms of ApoE ε2, ε3 and ε4 that differ from each other in a single amino acid. ApoE2 contains Cys at positions 112 and 158, whereas ApoE3 contains Cys at position 112 and Arg at position 158. Apo E4 contains Arg at both 112 and 158. A “domain interaction” occurs between Arg-61 and Glu-225 and this occurs more readily for ApoE4 than for ApoE3 because the interaction is promoted by Arg_{112}. Rodent ApoE is like human ApoE4 in that it contains Arg_{112}. On the other hand, rodent ApoE lacks Arg_{61} and therefore cannot participate in domain interaction and is functionally like ApoE3 (from Vance et al 2010).

The most common allele in European populations is ApoE ε3 with 70-80%, followed by ApoE ε4 with 10-14% and ApoE ε2 with 5-10% (Hagberg et al. 1995). The different amino acid substitutions at position 112 and 158 influence the functional and structural properties of the ApoE protein. ApoE3 and E4 bind to LDL receptors with similarly high affinity, whereas the binding of ApoE2 is 50 to 100 times weaker (Weisgraber et al. 1982). Cysteine to arginine substitution in ApoE2 at position 158 affects receptor-binding affinity by eliminating a salt bridge between arginine158 and asparagine154 and by forming of a new salt bridge between arginine150 and arginine154. This new bridge alters the conformation of arginine150 with respect to the other basic residues in the receptor-binding region reducing the ability of ApoE2 to interact effectively with LDL receptors (Dong et al. 1996) (Figure 6).

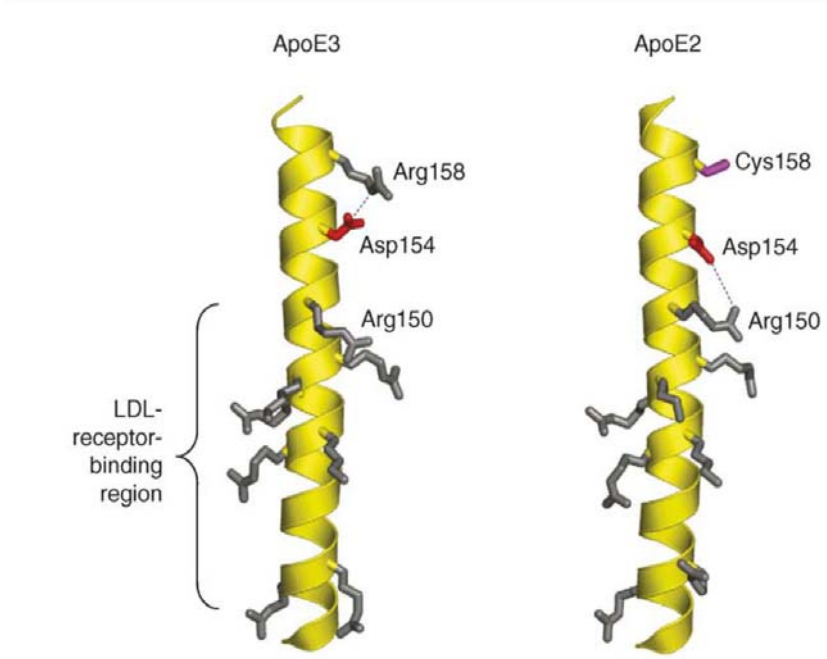

Figure 06 - Structural hallmarks of the ApoE isoforms.
Influence of amino acid position 158 on LDL-receptor-binding activity. The presence of cysteine or arginine at position 158 affects a key salt-bridge arrangement in ApoE3 and ApoE2, resulting in a different position of Arg150 that alters its ability to interact effectively with LDL receptors. In ApoE3, Arg158 forms a salt bridge with Asp154 (broken line). In ApoE2, by contrast, Asp154 forms a salt bridge with Arg150 (broken line), which lies in the basic LDL-receptor-binding region and changes its conformation and properties. (from Hatters et al. 2006)

1.2.3 The physiological function of ApoE

ApoE is a crucial regulator in the uptake of plasma cholesterol into the cell. High plasma cholesterol levels lead to pertubation of the arterial endothelium and account for a complex inflammatory response which cause sclerotic lesions in the intima. Hence, ApoE plays a key protective role in the pathogenesis of atherosclerosis (Curtiss et al. 2000). Transgenic mice over-expressing murine ApoE have lower plasma cholesterol levels and are resistant to diet-induced atherosclerosis (Shimano et al. 1992). Accordingly, ApoE null mice show elevated plasma cholesterol and increased susceptibility to diet-induced atherosclerosis (Zhang et al. 1992). In humans, the absence of ApoE or the presence of defective ApoE results in hyperlipoproteinemia, characterized by premature atherosclerosis and accumulation of plasma cholesterol (Ghiselli et al. 1981). Population studies have shown that the ApoE polymorphism has substantial effect on plasma lipids and lipoproteins, which are important risk factors for coronary heart diseases (Davignon et al. 1988). The influence of different ApoE isoforms on plasma cholesterol concentrations has been explained by several mechanisms, e.g. receptor binding affinities (Mahley an Ji et al. 1999) and dietary fat clearance (Weinstraub et al. 1987). However, ApoE2 is associated with type III hyperlipoproteinemia, a lipid disorder characterized by increased plasma levels of cholesterol and triglycerides (Mahley et al. 2001).

The most pronounced pathological effect attributable to ApoE polymorphism in humans is the association of ApoE4 with neurodegenerative diseases including Alzheimer disease (AD), the most common form of dementia in elderly (Selkoe et al. 2002). ApoE is a major apolipoprotein and a cholesterol carrier in the brain (Mahley et al. 1988) and in the case of the ε4 allele, a major risk factor for late-onset AD (LOAD) for the ε4 allele (Strittmatter et al. 1993). The ε4 allele frequency is ~10-14% in general populations but represents ~40% in patients with AD. Individuals with one

ε4 allele are three to four times more likely to develop AD than those without ε4 alleles (Corder et al. 1993). These observations suggest that the ε4 allele may be associated with accelerated neurodegeneration in the development and progression of several neurodegenative diseases (Bu et al. 2009).

1.2.4 Role of ApoE in bone metabolism

Apolipoprotein E is a plasma protein that is synthesized in various organs, including liver, brain, spleen, and kidney indicating a broad range of functions for this protein (Mahley et al. 1988). Besides the aforementioned involvement in atherosclerosis and neurodegeneration, ApoE also modulates bone metabolism. The nutritional composition of lipids and lipophilic vitamins is known to influence bone metabolism, in particular bone formation (Watkins et al. 2003). Growing experimental evidence suggest that lipid soluble vitamins, such as vitamin K, play an important role for osteoblastic function (Braam et al. 2003; Bolton-Smith et al. 2007). Chylomicrons (CM) and their remnants (CR) function as plasma carriers of these lipid constituents in the postprandial phase (Havel et al. 1997). The majority of CR is cleared by the liver via receptor-mediated endocytosis through LDLR and LRP1, which is mediated by ApoE (Mayley et al. 1999). Besides other tissues, bone is involved in the postprandial lipoprotein metabolism in mice. Osteoblasts participate in the CR clearance from the circulation, which has a direct impact on the secretory function of osteoblasts (Niemeier et al. 2008). Exogenously added ApoE enhances the uptake of vitamin K containing CR by human osteoblasts *in vitro*. This process is mediated by lipoprotein receptors, especially LRP1, that is found to be expressed at all stages of osteoblast differentiation (Niemeier et al. 2005). Vitamin K is required as a cofactor for the conversion of glutamyl (Glu) to γ-carboxyglutamyl (Gla) residues in certain specific proteins, often referred as Gla-proteins, such as osteocalcin

(Newman et al. 2002). Further studies in osteocalcin (OCN) deficient mice revealed an inhibitory effect on bone formation for this γ-carboxylation event (Ducy et al. 1996). Analogously, ApoE null mice display a high bone mass phenotype that is caused by an increased bone formation rate, whereas bone resorption is not affected. The absence of ApoE in mice leads to a decreased uptake of triglyceride-rich lipoproteins by osteoblasts, resulting in elevated levels of undercarboxylated osteocalcin in serum and subsequent increased bone formation (Schilling et al. 2005).

The specific induction of the ApoE gene expression during osteoblast differentiation along with the increased bone formation rate observed in ApoE null mice suggest that ApoE has a physiologic role in the regulation of osteoblastic function (Schilling et al. 2005). Human ApoE is polymorphic with three common isoforms (ApoE ε2, ε3, and ε4). Among these isoforms, ApoE2 has a 50-100 times reduced affinity to apolipoprotein receptors compared to the other isoforms (Weisgraber et al. 1982). Isoform-specific effects of the ApoE allele could be shown in cardiovascular diseases and neurological disorders. Interestingly, ApoE4 has been reported to be associated with reduced BMD and increased fracture risk (Shiraki et al. 1997; Kohlmeier et al. 1998; Dick et al. 2002; Lee et al. 2005). Although other studies could not confirm an association between ApoE4 and bone density or fracture risk (Heikkinen et al. 2000; Stulc et al. 2000; Sennels et al. 2003) there are still no published results on the analysis of the skeletal phenotype of mice expressing human ApoE ε2, ε3, and ε4, respectively.

1.3 Part 3 – bone metabolism and goal of the study

1.3.1 Assembly and metabolism of bone

The human skeleton has a total of 213 bones which are composed of two types of tissue, cartilage and bone, which are formed by chondrocytes and osteoblasts, respectively (Liu et al. 2008). Each bone constantly undergoes remodeling during life to help it adapt to changing biomechanical forces, as well as to remove old, micro-damaged bone and replace it with new bone to preserve bone strength (Clarke et al. 2008). The bones of the skeleton provide structural support for the rest of the body, permit movement and locomotion by providing levers for the muscles, protect vital internal organs and structures, provide maintenance of mineral homeostasis and acid-base balance, serve as a reservoir of growth factors and cytokines, and provide the environment for hematopoiesis within the marrow spaces (Taichman et al. 2005).

About 10% of bone is replaced each year with complete renewal every 10 years (Cohen et al. 2006). Bone remodeling is an ongoing dynamic process which involves the synthesis of organic matrix by osteoblasts and bone resorption by osteoclasts. General function of osteoblasts comprises synthesis of most proteins of the extracellular bone matrix, expression of genes necessary for calcification, and induction and downregulation of osteoclasts. Non-invasive assessment of bone turnover has markedly improved with the development of sensitive and specific markers of bone formation and bone resorption. Quantitative changes in skeletal turnover can be assessed by the measurement of serum and urinary biochemical bone markers. Biochemical monitoring of bone metabolism depends upon enzymes and proteins released during bone formation and resorption (Garnero et al. 1996). Alkaline phosphatase (ALP) and osteocalcin (OCN) are molecular markers for early and late stage of osteoblastic differentiation, respectively. As a product only sequestered by osteoblasts, plasma levels correlate with the activity of the cell

responsible for bone formation (Nakashima et al. 2003). Osteoclastogenesis is regulated by a sequential series of molecular factors which will be discussed in part later. The acidifying microenvironment necessary for bone resorption results from the action of cathepsin K, carbonic anhydrase II, and H^+-ATPase (Teitelbaum et al. 2000). Approximately 90% of the organic matrix of bone is type I collagen, a triple helical protein. Deoxypyridinoline (DPD) is a nonreducible pyridinium crosslink present in the mature form of collagen providing rigidity and strength. Because bone is by far the most abundant source of collagen matrix, urinary DPD coincide with osteoclast activity (Garnero et al. 1996).

Osteoblasts differentiate from mesenchymal stem cells through a series of progenitor stages to form mature matrix-secreting osteoblasts and are progressively transformed into osteocytes (Aubin et al. 2001). The osteoblast is defined by three major functions. First, it is responsible for the secretion of the bone extracellular matrix (ECM); second, it also expresses genes that are necessary and sufficient for the mineralization of this ECM; and third, the osteoblast is required for osteoclast differentiation and thereby a modulator for bone resorption (Glass et al. 2006). Commitment of mesenchymal stem cells to the osteoblast lineage requires the canonical Wnt/β-catenin-pathway and associated proteins (Logan et al. 2004). Mice harboring either gain-of-function or loss-of-function mutations in β-catenin in differentiated osteoblasts develop a high bone mass and a low bone mass phenotype, respectively. These phenotypes were primarily caused by altered bone resorption through the expression of OPG by osteoblasts (Glass et al. 2006). A similar bone phenotype could be shown in osteocyte-specific β-catenin-deficient mice. These mice show a low-bone-mass phenotype, associated with increased osteoclast number and activity that presumably is caused by significantly downregulated OPG expression by osteocytes (Kramer et al. 2010).

Osteoclasts are the only known cells to be capable of resorbing bone by attaching to the surface and secreting protons into an extracellular compartment formed under their ruffled border (Figure 7). This secretion is necessary for bone mineral solubilization and the digestion of the organic matrix by acid proteases (Rousselle et al. 2002). Activated multinucleated osteoclasts are derived from mononuclear precursor cells of the monocyte macrophage lineage (Boyle et al. 2003). Osteoclastogenesis is primarily regulated by the cytokines macrophage colony-stimulating factor 1 (M-CSF), RANKL, and by the decoy receptor OPG which are all secreted by osteoblasts (Lacey et al. 1998; Yasuda et al. 1998) (Figure 7). Analogously to bone formation and resorption, osteoclastogenesis can be determined by measuring osteoclastogenesis markers M-CSF, RANKL, and OPG in serum. RANKL belongs to the tumor necrosis factor (TNF) super-family and is critical signal to osteoclast progenitors for their differentiation into activated osteoclasts (Yasuda et al. 1998). Activated RANK induces the transcription factor c-Fos, which binds to DNA and upregulates several genes essential for mature osteoclasts capable of bone resorption (Takayanagi et al. 2002).The effects of RANKL on osteoclastogenesis can be fully blocked by OPG, also known as the osteoclastogenesis inhibitory factor, *in vitro* and *in vivo* (Lacey et al. 1998). M-CSF is required for the proliferation, survival, and differentiation of osteoclasts and their cytoskeletal rearrangement for bone resorption (Clarke et al. 2008).

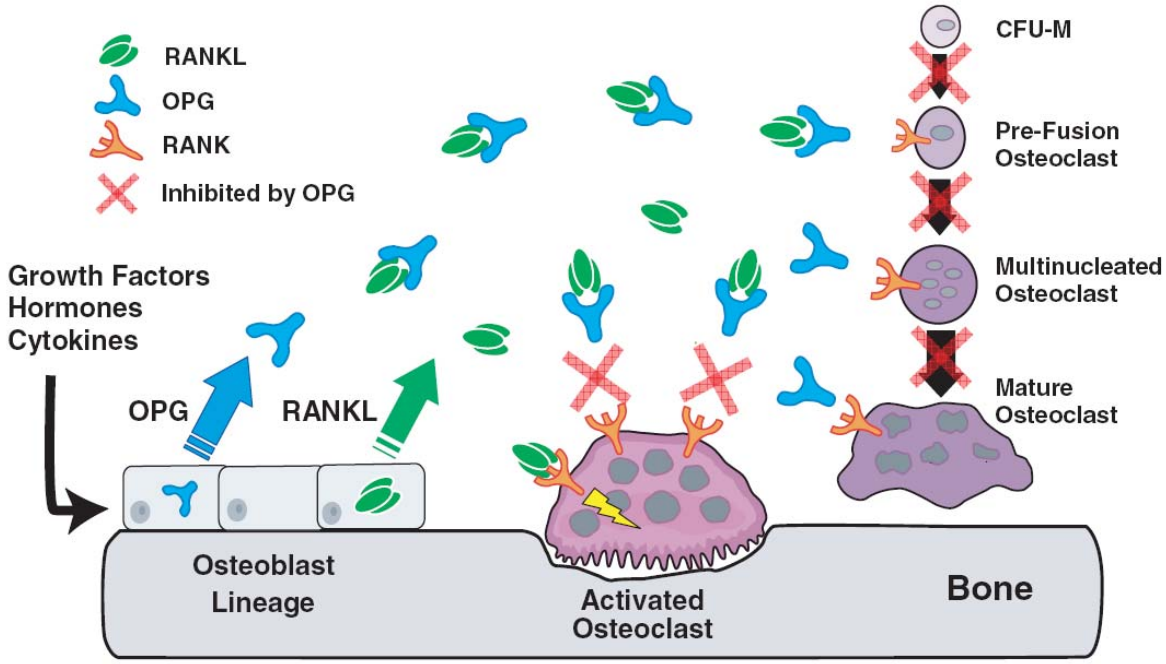

Figure 07 - Osteoclastogenesis is regulated by osteoblasts.

Mechanisms of action for Osteoprotegorin (OPG), receptor activator for nuclear factor κ B ligand (RANKL), and receptor activator for nuclear factor κ B (RANK). RANKL is produced by osteoblasts, bone marrow stromal cells, and other cells under the control of various proresorptive growth factors, hormones, and cytokines. Osteoblasts and stromal cells produce OPG, which binds to and thereby inactivates RANKL. In the absence of OPG, RANKL activates its receptor RANK, found on osteoclasts and preosteoclast precursors. RANK-RANKL interactions lead to pre-osteoclast recruitment, fusion into multinucleated osteoclasts, osteoclast activation, and osteoclast survival. Each of these RANK-mediated responses can be fully inhibited by OPG (from Kearns et al. 2008).

1.3.2 Wnt-signaling pathway in bone metabolism

Many current approaches to identify potential therapeutic targets for osteoporosis are focused on the Wnt/β-catenin-signaling pathway, which is of fundamental importance for osteogenesis (Baron et al. 2007). The Wnt co-receptor LRP5 has been demonstrated to participate in bone mass regulation (Krishnan et al. 2006) and was also found to associate with lumbar spine and femoral neck BMD in a collaborative large-scale meta-analysis of genome-wide association studies (Rivadeneira et al. 2009). It has been shown that loss-of-function and gain-of-function mutations in the human LRP5 gene are associated with osteoporosis-

pseudoglioma syndrome (OPS) and high bone mass (HBM) phenotypes, respectively (Gong et al. 2001; Little et al. 2002). Additionally, the low bone density phenotype is further exacerbated when loss of function in LRP5 is coupled to loss of an LRP6 allele, suggesting that both the LRP5 and LRP6 co-receptors are important in the Wnt-signaling effect on bone mass (Holmen et al. 2004). To date, no disorders have been associated with LRP6 genetic variation in humans. Mutant mice lacking LPR6 die during the perinatal period but mimic a phenotype out of a combination of various Wnt loss-of-function mutations (Pinson et al. 2000).

Wnt-signaling pathway is tightly regulated by members of several families of secreted antagonists, e.g. Dkk1 and SOST. Dkk1 is a soluble inhibitor of the Wnt/β-catenin-pathway and is regulated by BMPs (Grotewold et al. 2002). It is required for embryonic head and limb development and also regulates postnatal bone accretion and maintenance of bone mass mainly by binding to LRP5/6. Dkk1 binds to the first EGF-like domain of LRP5/6, which also represents the docking site for SOST and Wnt ligands, and promotes their internalization (Mao et al. 2001) (Figure 6B). Subsequently, these receptors are unavailable to form a complex with Fz and Wnt ligands which results in increased bone formation in a mutant mouse model target-deleted for Dkk1 (Morvan et al. 2006). Dkk1 null mice die perinatally and show severe developmental phenotypes, including head and limb dysmorphogenesis (Mukhopadhyay et al. 2001). A transgenic mouse mutant with reduced Dkk1 expression displays postnatal polysyndactyly, which can be partially rescued by the concomitantly reduced expression of LRP5/6 (MacDonald et al. 2004).

Another potent secreted Wnt-antagonist, SOST, also inhibits LRP5/6 co-receptor activity in osteoblasts by disruption the Fz/LRP5/6 complex formation leading to a reduction in bone mass with altered bone formation in overexpressing SOST-mice (Winkler et al. 2003). Consistent with the function of SOST as an

inhibitor of bone formation, SOST knockout mice have higher bone mass with increased BMD and bone strength (Li et al. 2008). Interestingly, overexpression of human SOST in transgenic mice resulted in an additional phenotype with fused or missing digits of the fore and hind limbs (Loots et al. 2005).

Besides the Wnt-signaling pathway, several other signaling pathway, such as transforming growth factor β including BMP, fibroblast growth factor (FGF), and Hedgehog signaling, have been shown to play an important role in regulating osteogenic differentiation. At the transcription level, several transcriptional factors have been identified as important regulators of osteogenic lineage commitment and terminal differentiation. These transcriptional factors include runt-related transcription factor 2 (Runx2), Osterix, activating transcription factor 4 (ATF4), and transcriptional modulator TAZ (Cohen et al. 2006; Deng et al. 2008).

1.3.3 The pathophysiology of osteoporosis

Osteoporosis is the most common skeletal disorder affecting 200 million individuals worldwide. It is characterized by low bone mass and microarchitectural deterioration of bone tissue which exposes patients to a greatly increased risk of bone fractures (Figure 8). Osteoporosis often is undertreated and under recognized, in part because it is a clinically silent disease until it manifests in the form of fracture (Lin et al. 2004).

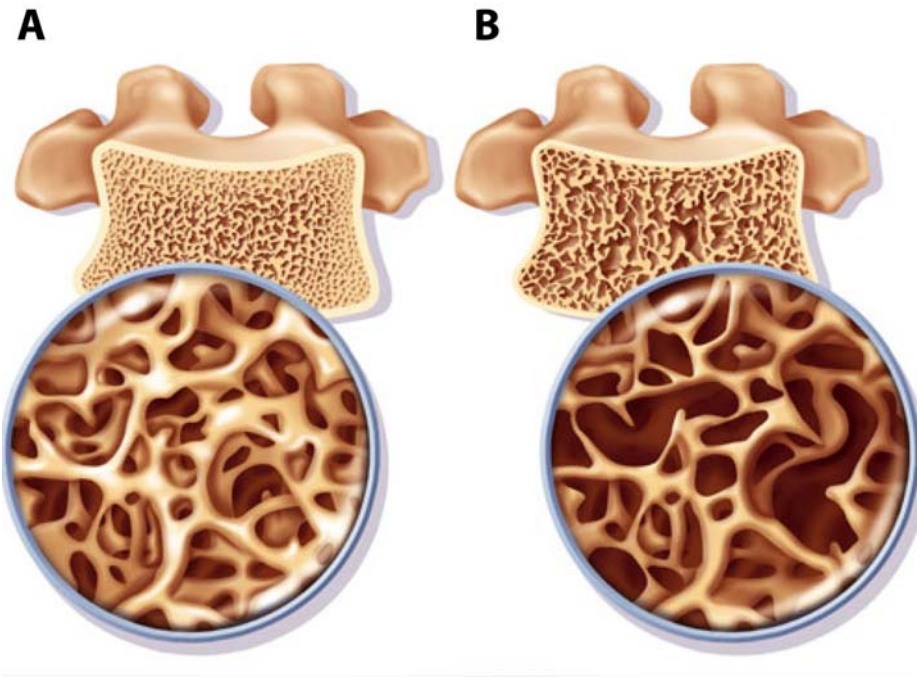

Figure 08 - Bone strength is influenced by bone density and quality.
(**A**) Illustration of normal healthy bone microarchitecture (**B**) and disturbed trabecular microarchitecture in a patient with osteoporosis in lumbar spine. (from www.webmd.com)

This disease is caused by a disruption of the fine equilibrium between the activity of osteoblast cells responsible for bone deposition and osteoclast cells for bone resorption (Heymann et al. 2000). Increased bone resorption or decreased bone formation may result in osteoporosis (Lin et al. 2004).

Osteoporosis can be categorized into two discrete types of involutional osteoporosis: postmenopausal (type 1; primary osteoporosis) and senile (type2; secondary osteoporosis) osteoporosis. Type 1, postmenopausal osteoporosis, that is associated with menopause and estrogen deficiency in women, is most apparent over the subsequent decade after menopause and involves mainly trabecular bone (Sipos et al 2009). Type 2 osteoporosis is age-related, which affects men and women older than 70 years and is characterized by continuously slow bone loss of both trabecular and cortical bone. Secondary causes include medications, endocrine disorders, chronic renal disease, hematopoietic disorders, immobilization,

inflammatory arthropathy, nutrition and gastrointestinal disorders, and connective tissue disorders (Lin et al. 2004)

1.3.4 Goal of this study

The function of LRP4, member of the multifunctional LDL receptor gene family, had been unclear until relatively recently. This receptor shares structural elements within the extracellular ligand binding domain with LRP5 and LRP6, two established Wnt co-receptors with important roles in osteogenesis. Growing experimental evidence of LRP4 in digit formation, kidney and tooth morphogenesis clearly indicates an involvement of this receptor in Wnt-signaling – a crucial pathway in bone metabolism. In addition, overlapping developmental phenotypes in genetically manipulated mice of SOST and Dkk1 could be observed. Moreover, LRP4 and Wnt-signaling antagonist SOST has been associated with lumbar spine and femoral neck BMD – the key trait in osteoporosis.

Although single nucleotide polymorphisms (SNPs) of ApoE could not been associated with femoral neck and lumbar spine BMD and increased fracture risk in the meta-analysis of genome-wide association studies, the high-bone-mass phenotype of $ApoE^{-/-}$ mice clearly demonstrates an involvement of ApoE in bone metabolism. To date, the effects of the different ApoE polymorphisms ($\varepsilon 2$, $\varepsilon 3$, and $\varepsilon 4$) on bone metabolism remain controversial. However, the effects of the different ApoE polymorphisms have not been accurately characterized in a mouse model until now.

In this study we wanted to investigate the function of LRP4 in bone metabolism, using a LRP4 mutant mouse strain expressing the extracellular domain of LRP4 only, and to determine the effects of the ApoE polymorphisms, using mice expressing human ApoE $\varepsilon 2$, $\varepsilon 3$, and $\varepsilon 4$, respectively.

2 Materials and methods

2.1 LRP4 EC-Stop (ECD) plasmid construction

LRP4 ECD mice were generated by introducing a stop codon into the exon 36 of LRP4 gene, resulting in the extracellular truncation of the protein and the loss of the transmembrane and intracellular domains of LRP4 (Figure 9B). This strategy was chosen, because it prevents the production of a membrane-anchored receptor and eliminates any possibility of any residual functional activity through alternative splicing of the extracellular domain or the use of alternative promoters for transcription initiation (Johnson et al. 2005).

A replacement-type vector was constructed using homology amplified long and short arms by polymerase chain reaction (PCR) from ES cell genomic DNA using long-range PCR (Takara Biochemical, Inc., Berkeley, CA) with the following primers:

Long arm:

KI3 (5'-CCACCACCTGCAGGGTATACTGAGGAGTCCACCGATGGCATAGCTG-3') and

KI4 (5'-CACCACCTGCAGGCGGCCGCGAATATGATATCATGTCAATACTAGAG ACTTA CC-3')

Short arm:

MEJ76 (5'-CCACCACTCGAGCCTGTGGACCTTCCTATAAGTCAACTTCC-3') and

MEJ77 (5'-CCACCACTCGAGGGTTGACTGCTAACAATCAGAGCAGGCTG-3')

Primers were used as 5' and 3' primers, respectively, to amplify the long and short arm.

The short arm was cloned into pJB1 at the XhoI site. To introduce a stop codon into exon 36 of LRP4, the long arm was mutated using the following primers (Figure 9A):

MEJ143 (5'-CCTAGGTGAAGGACTGTAAGTCAGCTATGCCATC-3') and

MEJ144 (5'-GATGGCA TAGCTGACTTACAGTCCTTCACCTAGG-3').

The mutated long arm and the bovine growth hormone 3' untranslated region were cloned into the pJB1-short arm containing plasmid using NotI to generate the targeting vector. Recombinant ES cell clones were generated by electroporating the linearized vector into SM1 ES cells. Clones were selected by PCR, verified by Southern blotting. To minimize the effects of genetic drift and vertical inbreeding, mice from the entire LRP4 ECD heterozygote pool of our colony on 129SvEv x C57BL/6 hybrid backgrounds were crossed to produce wild type and LRP4 ECD littermate controls.

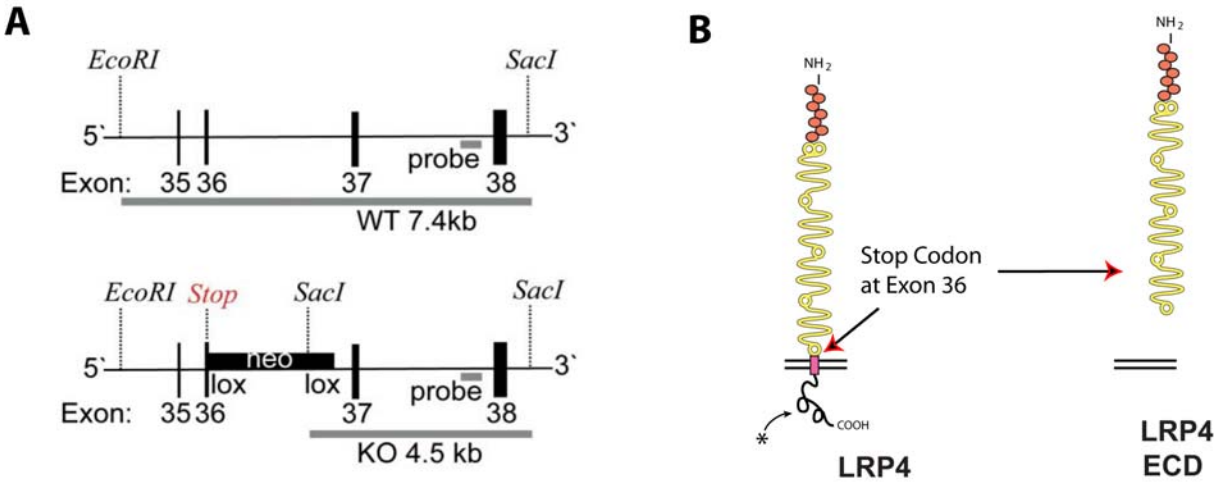

Figure 09 - Cloning strategy to generate LRP4 extracellular domain (ECD) mice.
A premature stop codon was introduced into murine exon 36 (**A**), which encodes the transmembrane domain of LRP4. (**B**) Illustration of structural organization of LRP4 after introduction of a stop codon into exon 36 (from Johnson et al. 2005).

2.1.1 Genotyping of LRP4 WT/ECD

To verify the specific genotype of mice, the following PCR reaction was used (Soriano Method):

1 reaction (25µl total volume, components were added in the indicated order)

14.7µl	water
2.5µl	10X Soriano Buffer
2.5µl	dNTPs (10mM)
2.5µl	DMSO
1.25µl	BSA (1.6mg/ml)
0.2µl	5'primer (100µM)
0.2µl	3'primer (100µM)
0.15µl	polymerase (ExTaq 5U/µl)
1µl	DNA sample

PCR reaction conditions

1. Melting	94°C	2:00
2. Annealing	60°C	2:00
3. Extension	65°C	3:00
4. Melting	94°C	0:30
5. Annealing	60°C	0:30
6. Extension	65°C	2:00
7. Extension	65°C	10:00
8. Storage	4°C	∞

Repeat steps 4-6 for 45 cycles.

Following primer sets were used for the aforementioned PCR reaction in C1000 Thermal Cycler (BioRad) to verify the genotype:

LRP4*wildtype*

5’ primer: MEJ155 - 5’-CCCAGCTGGGCCTCTGTGCACATTCCAATG-3’

3’ primer: MEJ166 - 5’-CCATGGCCTCTGCATTAGTTCTTGCTCTC-3’

LRP4*EC Stop (ECD)*

5’ primer: MEJ156 - 5’-CTCTGAAAGGGATGCCCAGCTGGGCCTCTG-3’

3’ primer: MEJ267 - 5’-CGATGGCATAGCTGACTTA-3’

2.2 Human ApoE isoform plasmid construction

ApoE targeted replacement mice express the human ApoE protein at physiological levels and retain the endogenous regulatory sequences required for modulating ApoE expression. These mutant mouse lines, originally generated in the Maeda lab, were purchased from Taconic (Taconic Laboratories, Hudson, NY). All three ApoE mouse lines were created by gene targeting and carry one of the three human alleles (ApoE ε2, ε3, or ε4) in place of the endogenous murine ApoE gene. Therefore the mice have identical levels of ApoE expression in all normally ApoE occurring mouse cell types (Sullivan et al. 1997; Sullivan et al. 1998; Knouff et al. 1999)

The targeting construct was made by inserting into a pPNT vector (Tybulewicz et al. 1991), a 4.1kb *Sac*I human genomic fragment isolated from a plasmid, pHEG-1 (Simonet et al. 1990). This fragment contains the 3´ part of intron 1 (723 base pairs), exons 2–4 of the human ApoE2, 3, 4 gene, respectively, and 1.5kb of 3´-flanking DNA. A 5.3kb *Eco*RI-*Sac*I strain 129 mouse genomic fragment

containing sequences upstream of the mouse ApoE gene including exon 1 and the 5´ part of intron 1 (376 base pairs) was inserted 5´ to the human ApoE3 fragment. A 1.4kb *Pvu*I-*Kpn*I strain 129 mouse genomic fragment containing the 3´-half of exon 4 and 3´-flanking sequence was inserted downstream of the neomycin-resistant gene in pPNT (Sullivan et al. 1997) (Figure 12).

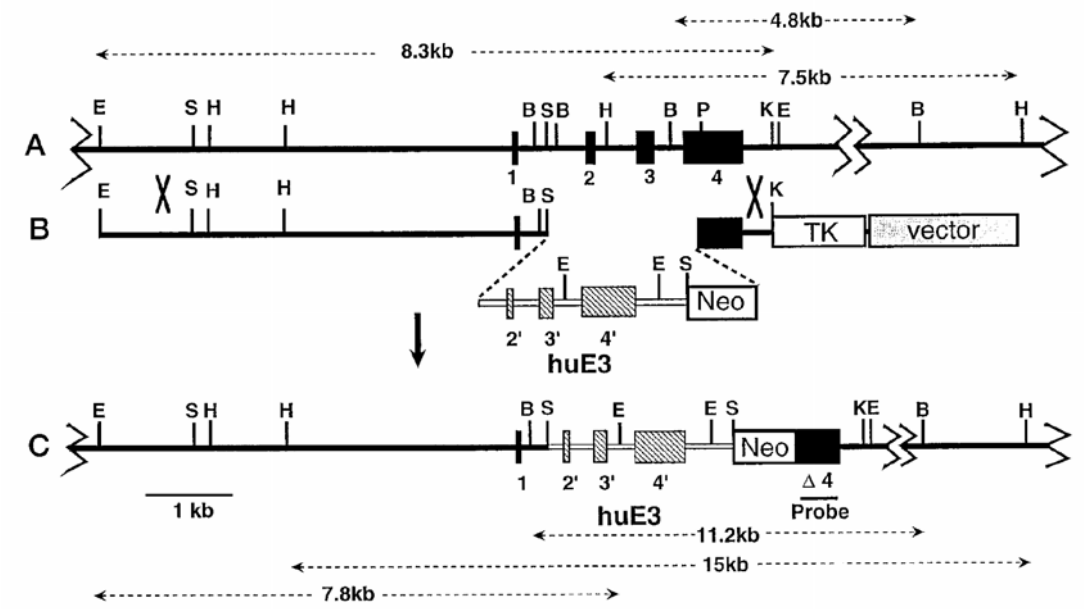

Figure 10 - Cloning strategy to generate human ApoE knockin mice.

(**A**) Scheme of the genomic organization of the mouse ApoE gene containing exons 1–4 (*black boxes*). (**B**) The ApoE3 targeting construct containing the 5´ and 3´ arms of mouse homology (*black line* and *boxes*) interrupted by the human ApoE3 gene (*hatched boxes* 2´, 3´, and 4´, labeled *huE3*). The neomycin-resistant (*Neo*) and thymidine kinase (*TK*) genes are for selection of the targeted ES cells, and pPNT is the plasmid vector. (**C**) The resulting chimeric gene now encoding human ApoE3. The mouse exon 4 probe (*Probe*) was used to detect the targeted allele. Sizes of diagnostic fragments are shown (*dashed lines*). Sites are as follows: *E*, *Eco*RI; *S*, *Sac*I; *H*, *Hin*dIII; *P*, *Pvu*I; *K*, *Kpn*I; *X*, *Xba*I; *B*, *Bam*HI (from Sullivan et al. 1997). ApoE2 and ApoE4 targeting constructs were generated using the same procedure.

A subclone (BK4) of mouse strain 129 embryonic stem (ES) cell line, E14TG2a, was cultured and electroporated with the human respective ApoE targeting construct. Targeted ES cell clones were identified by Southern blot

analysis and chimeras were generated and mated with C57BL/6J (B6) mice (Sullivan et al. 1997).

2.2.1 Genotyping of ApoE human knockin animals

To verify the homozygosity of the human ApoE knockin alleles, the following PCR reaction was used. (Soriano Method):

1 reaction (25µl total volume, components were added in the indicated order)

14µl	water
2.5µl	10X Soriano Buffer
2.5µl	dNTPs (10mM)
2.5µl	DMSO
1.25µl	BSA (1.6mg/ml)
0.5µl	5'primer (100µM)
0.5µl	3'primer (100µM)
0.25µl	polymerase (ExTaq 5U/µl)
1µl	DNA sample

PCR reaction conditions

1. Melting	94°C	2:00
2. Annealing	60°C	2:00
3. Extension	65°C	3:00
4. Melting	94°C	0:30
5. Annealing	60°C	0:30
6. Extension	65°C	2:00
7. Extension	65°C	10:00
8. Storage	4°C	∞

Repeat steps 4-6 for 45 cycles.

Following primer sets were used for the aforementioned PCR reaction in C1000 Thermal Cycler (BioRad) to verify the homozygosity of the human knockin alleles:

ApoE*wildtype*

5’ primer: UB776 - 5’-GCCTAGCTGTGTACAAGGCA-3’

3’ primer: UB777 - 5’-TTGATTCTCCTGGGCCACTG-3’

ApoE*human knockin*

5’ primer: UB788 - 5’-GCAGCCTCTGTTCCACATACACT-3’

3’ primer: UB777 - 5’-TTGATTCTCCTGGGCCACTG-3’

To verify the specific ApoE isoform, PCR products were extracted from gel and purified using Qiaquick gel extraction kit (Qiagen) according to manufacturer’s instructions. Samples were sent for sequencing (McDermott Center, UT

Southwestern) and analyzed using Basic Local Alignment Search Tool (National Center for Biotechnology Information, NCBI).

2.3 Animal terms

All animals were maintained in the UT Southwestern animal facility with 12h light/12 h dark cycle and fed a standard rodent chow diet (Diet 7001, Harlan Teklad, Madison, WI) with access to water ad libitum. At twelve weeks, experimental mice were fasted for 5 h prior to collection of serum and urine. After sample collection, the mice were injected intraperitonially with 30mg/kg calcein (Sigma Alderich, St. Louis, MO). This procedure was repeated after one week. Nine days after the first injection mice were euthanized with isoflurane (Butler), skeletons or single bones, e. g. calvaria, tibia, and femur, were extracted. Upon sacrifice, mouse skeletons were fixed in 4% PBS-buffered formaldehyde (PBS; Dulbecco´s phosphate buffered saline from Cellgro; PFA; Electron Microscopy Sciences) over night at 4 °C followed by an over night incubation in 70% ethanol, and finally stored in 80% ethanol. Single bones were used to extract protein and ribonucleic acid (RNA), respectively, and processed as described below. All procedures were performed in accordance with the protocols approved by the Institutional Committee for Use and Care of Laboratory Animals of the University of Texas Southwestern Medical Center at Dallas (IACUC).

2.4 Extraction of protein and RNA from primary bone

For further analysis, calvaria, femur, and tibia were extracted and cleaned by removing connected tissues with a scalpel.

To extract protein, calvaria, femur, and tibia were ground in a mortar in liquid nitrogen, separately, followed by 3min of bead shaking in 200µl 50 mM Tris-HCl buffer, pH 7.5 containing 150mM NaCl, 1mM $MgCl_2$, 1mM $CaCl_2$, 1% Triton X-100,

protease inhibitors (Roche), and phosphatase inhibitor (Thermo Scientific) at 200Hz (TissueLyser2, Qiagen). After homogenizing the bone tissue, samples were kept on ice for 30min, centrifuged, and liquid supernatant was transferred to a new tube for protein determination according to Lowry (D_c Protein Assay, BioRad). For the immunoblotting of proteins from primary bone samples and cultured cells were separated on a 4-15% polyacrylamide gel (BioRad) and transferred onto nitrocellulose membranes at 90V for 90min. Western blot analysis of proteins was carried out with anti-LRP4 (584c), anti-alkaline phosphatase, anti-total β-catenin, and anti-unphosphorylated β-catenin antibodies and detected by enhanced chemiluminescence (Thermo Scientific).

To extract total RNA from bone (calvaria, femur, and tibia), samples were separately ground in a mortar in liquid nitrogen followed by 12min of bead shaking in 1ml Trizol® reagent (Invitrogen) at 200Hz. After homogenizing the bone tissue, 200µl chloroform was added, shaken vigorously for 15sec, and incubated for 3min at room temperature (RT). Samples were centrifuged at 12 000g at 4° for 15min, aqueous phase was transferred to a fresh tube and 500µl isopropanol was added. After 10min incubation at RT, samples were centrifuged at 12 000g at 4° for 10min and supernatant was discarded. 1ml 70% EtOH was added to samples and centrifuged at 7 500g at 4° for 5min. EtOH was discarded and RNA pellet was dissolved in 100µl DEPC water. RNA concentration was measured using Ultrospec3100pro (Amersham Biosciences).

The RNA was treated with DNase I (Ambion) to exclude potential contamination by DNA. 90µl RNA was treated with 1xDNase I buffer and 1µl DNase I (Ambion) at 37° for 30min. After incubation, DNases were inactivated by DNase inactivation reagent (Ambion) and incubated at RT for 2min. Samples were spun down and supernatant was transferred into a new tube. 2µg of DNA-free RNA were

reverse-transcribed using TaqMan Reverse Transcription Reagents (Applied Biosystems).

Reverse transcription for RT-PCR was set up in the indicated order:

RNA (DNA-free)	2µl
Water	36,5µl
10x RT-buffer	10µl
25mM $MgCl_2$	22µl
dNTP	20µl
50mM random hexamer	5µl
RNase inhibitor	2µl
Multiscribe RT	2,5µl

The three step reaction was performed in C1000 Thermal Cycler (BioRad) at 25° for 10min, 48° for 30min, and 95° for 5min, respectively.

Quantitative real-time PCR (RT-PCR) analysis was performed using the ABI PRISM 7900HT Sequence Detection System (Applied Biosystems). Each 20ml reaction contained 20ng/ml cDNA, 2.5mM forward and reverse primers, and 10ml of 2x SYBR Green PCR Mater Mix (Applied Biosystems).

Following primer sets were used:

36B4 (housekeeper)

5’-CACTGGTCTAGGACCCGAGAAG	3’ (forward)
5’-GGTGCCTCTGGAGATTTTCG	3’ (reverse)

β-catenin

5’-CCTCCCAAGTCCTTTATGAATGG	3’ (forward)
5’-CCGTCAATATCAGCTATTGCTCTT	3’ (reverse)

LRP5

5’- ACCCGCTGGACAAGTTCATC	3’ (forward)
5’- TCTGGGCTCAGGCTTTGG	3’ (reverse)

LRP6

5’-AAATTGACATGACTGGTCGAGAAG	3’ (forward)
5’-TTCAGCTCCTTTACTGCATGGA	3’ (reverse)

Dkk1

5’-TGTCAGCTCAATCCCAAGGAT	3’ (forward)
5’-CACTCCAGAGCTTTTGGAAGGT	3’ (reverse)

Dkk2

5’-GCAGAATTGTCTCAGATTGCAAA	3’ (forward)
5’-GCTCATCCCGTCATTCAGTTC	3’ (reverse)

SOST

5’-CCCTGACCTGGCCACTGA	3’ (forward)
5’-AGTTCCGGTCCCTATTTTACAAAGA	3’ (reverse)

2.5 Generation of a primary osteoblastic lineage

Primary osteoblasts were obtained by sequential collagenase digestion of calvariae from 3–4 day old wildtype C57Bl/6 mice. After incubation for 40min in αMEM containing 0,1mg/ml collagenase P–2.5% trypsin at 37°C, shaking, calvaria were washed in αMEM, cut in pieces and transfered in αMEM containing 0,1mg/ml collagenase P-10% trypsin for 1 hr at 37°C. Digestion was stopped by addition of 10 volumes of αMEM with 10% FCS. Osteoblast differentiation was induced at 80% confluency in αMEM containing 10% fetal bovine serum, 50mg/ml ascorbic acid and 10mM β-glyerophosphate. At day six of differentiation, total cell proteins were isolated and subject to western blot analysis.

2.6 Production of recombinant proteins and binding assay

HEK293A cells were transfected with pcDNA3.1-AP, pcDNA3.1-RAP-AP, pcDNA3.1-Wise-AP, pcDNA3.1-R-spondin2-AP, pcDNA3.1-Dkk1-AP, or pcDNA3.1-SOST-AP constructs using FuGENE 6 (Roche, using manufacturer's protocol) in DMEM plus 0.2% BSA medium to produce conditioned media containing AP or AP-tagged recombinant proteins. After 48h transfection, media were collected and the production levels of AP and AP-tagged proteins in the media were determined by AP activity assay using p-Nitrophenyl phosphate (Calbiochem, according to manufacturer´s instruction) as a substrate.

To investigate the binding of AP-tagged proteins to LRP4 in a cell-free system, media containing of the LRP4 ectodomain fused to the constant region of Immunoglobulin G (LRP4ecto-Fc) was produced by transfection of HEK293A cells with pcDNA3.1-LRP4ecto-Fc in DMEM plus 0.2% BSA medium. The medium containing LRP4ecto-Fc was incubated with protein A-agarose beads (Sigma) at 4°C

for 2 h to bind LRP4ecto to the beads. Equal volumes of media containing AP or AP-tagged proteins were pre-cleared with protein A-agarose beads at 4°C for 2 h and then incubated with the LRP4ecto-bead conjugates at 4°C overnight. The conjugates were washed four times with PBS, resuspended in 40 ml Laemmli sample buffer, and western blotting was performed using anti-AP antibody (Sigma).

To investigate binding of AP-tagged proteins to LRP4 in a cell system, HEK293A cells were transfected with pcDNA3.1-LRP4 full length constructs for 48h, washed once with PBS plus 0.1% BSA, and incubated in equal volumes of media containing AP or AP-tagged proteins at 37uC for 1h. The cells were washed once with PBS, incubated with 250mM cross-linker dithiobis[succinimidylpropionate] (Pierce), at RT for 30min, harvested, washed three times with PBS, and lysed in 50mM Tris-HCl buffer, pH 7.5 containing 150mM NaCl, 1mMMgCl2, 1mM CaCl2, 1% Triton X-100, and protease inhibitors (Roche). After determination of protein concentration by Lowry assay, equal protein amounts of the cell lysates were subjected to immunoprecipitation using anti-AP antibody and protein A-agarose beads. Immunoprecipitates were boiled in SDS sample buffer containing 5% β-mercaptoethanol and western blotting was performed using anti-LRP4 antibodies derived against the carboxy terminus and the murine LRP4 ectodomain, respectively.

2.7 Measurement of bone formation and resorption markers

All serum and urine samples were stored at minus 20°C immediately after the blood draw and were not thawed prior to analysis. To determine bone formation markers, osteocalcin and alkaline phosphatase levels were determined in serum. Osteocalcin levels were measured using a two-site immunoradiometric assay (Immutopics) according to the manufacturer's instructions. Alkaline phosphatase activity in serum,

was measured using the pNPP method. Briefly, 5µl of serum were mixed with 50ml of substrate solution containing 2mg/ml of p-Nitrophenyl Phosphate (Sigma) in alkaline buffer solution (Sigma). After incubation at 37°C for 15min, the reaction was stopped by adding 500µl of 0.5M NaOH and the absorbance at 405nm was measured. Alkaline phosphatase activity was determined by using p-nitrophenol solution (Sigma) as standard substrate. To determine bone resorption markers, deoxypyridinoline (DPD) levels were quantified in urine and normalized against urinary creatinine levels. DPD and creatinine levels were measured by using MicroVue DPD (Quidel) and MicroVue creatinine (Quidel), respectively, using manufacturer's protocol. Osteoclastogenesis markers, OPG and RANKL levels were determined in serum by using Quantikine immunoassay (R&D Systems) according to manufacturer's instructions.

2.8 µCT analysis of femoral bone and lumbar spine

Whole-animal contact radiographies were performed using an x-ray cabinet (Faxitron). Upon sacrifice, mouse skeletons were fixed in 4% PBS-buffered formaldehyde over night at 4 °C followed by an over night incubation in 70% ethanol, and finally stored in 80% ethanol. In order to analyze the bone microstructure, the femora and lumbar spine were scanned (55 kV/145 µA) in a micro computer tomograph µCT40 (Scanco Medical) with a voxel size of 12 µm. Five samples were scanned simultaneously using a specially built sample-holder with an integrated mineralization phantom which enables immediate bone mineral density evaluation. At the same time, histomorphometric data for cortical thickness (µm), cortical area (mm^2), cortical and trabecular mineralization (mg/ml), and femur length (mm) were determined in the scanned samples. For respective LRP4 ECD mice, analysis of bone volume (BV/TV; %), trabecular thickness (TbTh; µm), trabecular number (TbN; mm), and trabecular

separation (TbSp; µm) was performed in lumbar spine. The raw data were manually segmented and analyzed with the µCT Evaluation Program V4.4A (Scanco Medical).

2.9 Histological analysis of lumbar spine

For comparative quantitative histomorphometry, the undecalcified lumbar spines of respective ApoE mice were embedded in methylmethacrylate after dehydration and 5 µm sections were cut in sagittal plane on a rotation microtome (Cut 4060E, MicroTech) as described (Amling et al. 1999). Sections were stained with toluidine blue and with modified von Kossa/van Gieson. Analysis of bone volume (BV/TV; %), trabecular thickness (TbTh; µm), trabecular number (TbN; mm^{-1}), trabecular separation (TbSp; µm), and trabecular bone formation rate (BFR/BS; µm 3/µm2/year) was performed according to standardized protocols of the American Society for Bone and Mineral Research using the Osteomeasure histomorphometry system (Osteometrix) in a blinded fashion. For the assessment of dynamic histomorphometric indices, mice were injected twice with calcein label as described above. Fluorochrome measurements were made on two nonconsecutive 12µm thick sections per sample that were mounted unstained in Fluoromount (Electron Microscopy Sciences).

2.10 Biomechanical analysis of femoral bone

Biomechanical stability of the femora was determined by three-point-bending assays using a commercial high precision instrument (Z2.5/TN 1S Zwick, Ulm, Germany). In brief, the ends of the bone were supported on two fulcra separated by 7 mm. With the posterior aspect of the femur resting on the fulcra, a load was applied from above to the anterior diaphysis midway between the two fulcra, at a constant speed of 3 mm/min to failure. A chart recorder was used to generate a force-deformation curve.

Maximum force (fmax, N) and energy absorption when reaching maximum force (N x mm) were evaluated.

3 Results

3.1 Part 1 – LRP4 in bone metabolism

3.1.1 LRP4 interacts with Dkk1 and SOST *in vitro*

Both Dkk1 and SOST modulate Wnt-signaling by binding to EGF-like repeats of LRP5 and LRP6. Subsequently these receptors are unavailable to form a complex with Fz and Wnt ligands to activate Wnt-signaling pathway (Morvan et al. 2006). The extracellular domains of LRP4, LRP5 and LRP6 are highly conserved (Johnson et al. 2005), raising the possibility that the spectrum of ligands that bind to LRP5/6 and LRP4 might overlap. In order to test for a physical interaction between Dkk1 and LRP4 as well as SOST and LRP4, we performed two types of in vitro binding assays.

First, HEK293A cells transfected with LRP4 were incubated with conditioned media containing the alkaline phosphatase (AP)-tagged putative LRP4 ligands (Figure 11A). The 39kDa receptor-associated protein (RAP), a chaperone for LDLR gene family members, is known to bind to LRP4. Previously it was shown that Wise interacts with LRP4, while another modulator of the Wnt signalling pathway, R-spondin2 (RS2) does not (Ohazama et al. 2008). Thus, RAP and Wise served as positive controls, RS2 and non-tagged AP as negative controls for these assays. AP-fusion proteins of controls and the putative ligands Dkk1 and SOST were pulled down with an antibody against AP and immunoblotted with an anti-LRP4 antibody to detect co-precipitated receptor (Figure 11B). In a complementary, converse cell free assay, the LRP4-Fc fusion protein was immobilized on Protein A-agarose and incubated with the AP-tagged putative ligands and controls. LRP4 bound ligands were then detected by immunoblotting against AP (Figure 11C). For the first time it

could be shown that LRP4 binds the Wnt-signaling inhibitors Dkk1 and SOST. Both assays showed the same binding patterns for LRP4 *in vitro* (Figure 11B and C).

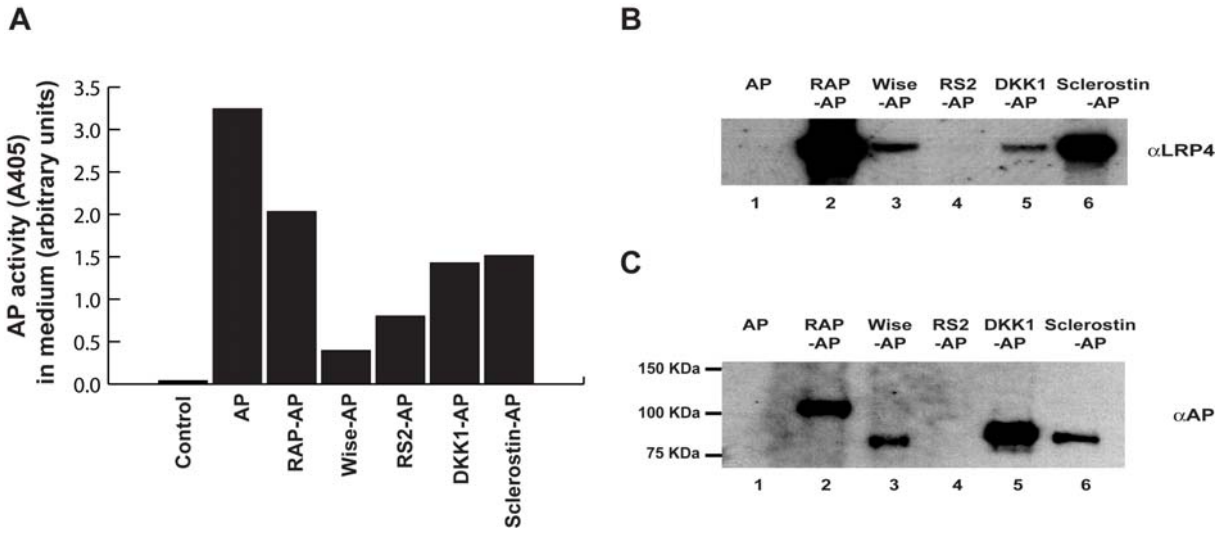

Figure 11 - LRP4 interacts with Dkk1 and SOST *in vitro*.

(**A**) HEK293A cells were transfected with alkaline phosphatase (AP) as a control and with AP-tagged confirmed and putative low-density lipoprotein receptor-related protein 4 (LRP4) ligands. The relative abundance of the respective ligands in the cell culture supernatant is shown as AP activity (arbitrary units). (**B**) Conditioned media containing the indicated AP-fusion proteins were incubated with HEK293A cells overexpressing LRP4. After binding and crosslinking, AP-fusion proteins were immunoprecipitated, and coprecipitated LRP4 was detected by immunoblotting. RAP constitutively interacts with LDL receptor family members and serves as a positive control. R-spondin2 served as a negative control. LRP4 coprecipitates with dickkopf 1 (Dkk1) and sclerostin (SOST) AP fusion proteins (**C**) In a cell free assay, soluble LRP4 ectodomain-Fc fusion protein was conjugated to protein A-agarose, incubated with media containing the AP-tagged putative LRP4 ligands and LRP4 bound ligands were then detected by immunoblotting against AP.

3.1.2 LRP4 is expressed in bone and osteoblasts

More and more experimental evidence suggest the Wnt-signaling pathway as one the major pathways involved in osteogenesis. Both SOST and Dkk1 bind to LRP5/6, which play critical roles in the Wnt/β-catenin signal transduction in osteoblasts and therefore on the differentiation and activity of osteoclasts. In light of our finding that Dkk1 and sclerostin bind to LRP4, we next analyzed whether LRP4 is also expressed in bone.

To prove RNA expression levels of LRP4 quantitative RT-PCR blot analysis were conducted. Murine embryonic brain (E18) from LRP4 null mice and wild type littermates served as a negative and positive control for the RT-PCR and immunoblots, respectively (Figure 12A, B). RT-PCR measurements revealed mRNA levels in murine calvaria and femoral bone (Ct levels 27,9±0,06 for brain; 28,8±0,10 for calvaria; 31,3±0,21 for femur) (Figure 12A). An agarose gel of the PCR products confirmed LRP4 RNA expression levels (Figure 12B). No RNA expression could be detected for the LRP4 null mice in which the promoter and exon 1 of LRP4 have been deleted (Dietrich et al., 2010).

A

Gene	WT E18 Brain Ct (avg. ± S.D.)	Lrp4-/- E18 Brain Ct (avg. ± S.D.)	WT adult calvaria Ct (avg. ± S.D.)	WT adult femur Ct (avg. ± S.D.)
Lrp4	27.9 ± 0.06	N.D.	28.8 ± 0.10	31.3 ± 0.21
36B4	20.7 ± 0.02	21.0 ± 0.01	24.4 ± 0.01	25.9 ± 0.03

B

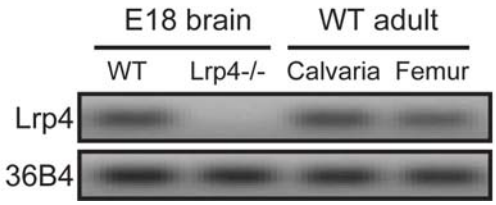

Figure 12 - RNA expression of LRP4 in calvaria and femoral bone

(**A**) Total RNA was extracted from embryonic brain (E18), calvaria and femur cortical bone of 10-week old adult mice. Quantification of LRP4 and control (36B4) mRNA was performed by real-time PCR. Results represent the average of cycle threshold (Ct) ±S.D. in triplicate. (**B**) Agarose gel of the PCR products from the experiment shown in (**A**).

After proving LRP4 RNA expression levels, protein levels were detected by a polyclonal antibody derived against the recombinantly expressed LRP4 ligand

binding domain (Figure 13B). As expected, LRP4 null animals showed no expression of LRP4 protein (Figure 13A), whereas protein was present in wild type calvaria and femur (Figure 13A). Moreover, LRP4 protein could be detected in primary calvarial osteoblasts from newborn wild type mice that had undergone six days of in vitro differentiation with ascorbate and β-glycerolphosphate (Figure 13B).

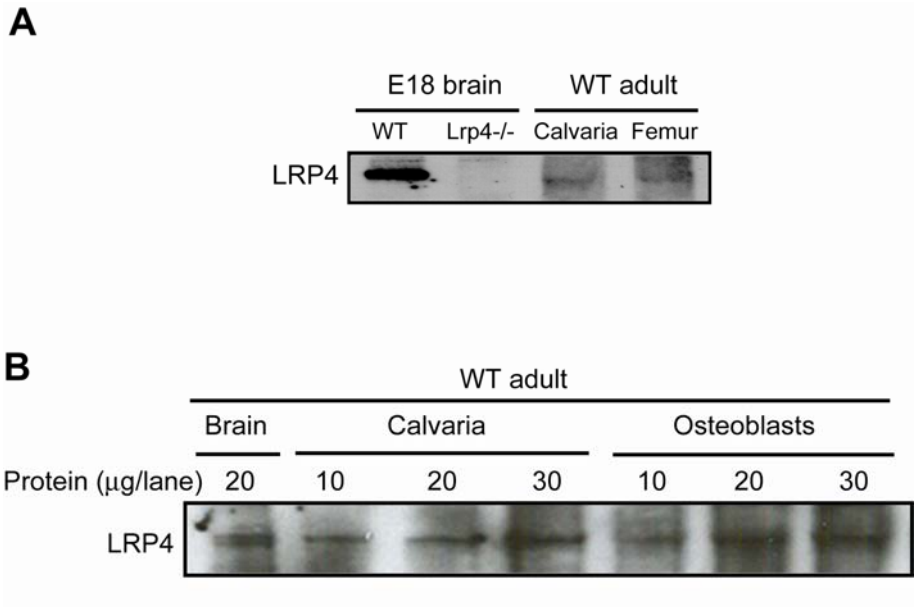

Figure 13 - Protein expression of LRP4 in bone and primary osteoblasts.
(**A**) Extracted proteins were subjected to immunoblotting with an antibody against LRP4. (**B**), Protein extracts from primary osteoblast cultures after 6 days of in vitro differentiation were subjected to anti-LRP4 immunoblotting. Brain and calvarial extracts are shown as controls.

Taken together, these data demonstrate that LRP4 is expressed in murine bone and, more specifically, in osteoblasts.

3.1.3 Functional LRP4 deficiency results in impaired skeletal growth and reduced trabecular bone volume

In order to investigate the physiological significance of the expression of LRP4 by osteoblasts, we performed micro computer tomography (µCT) of the femur and lumbar spine vertebrae of LRP4 ECD mutant mice and wild type littermates. Ten week old male animals were analyzed (n=6 per genotype for µCT). MicroCT 3D and 2D reconstruction of the femur did not reveal striking differences in the overall morphology of the bones (Figure 14A, B), but showed that the reduction of total body weight (25,7 ±1,3g for WT and 20,3 ±1,4g for LRP4 ECD littermates; Figure 14C) was accompanied by a significant reduction of femur length (13,5 ±0,3mm vs 12,5 ±0,2mm p=0,0001; Figure 14D) and a clear, albeit statistically non-significant trend towards a reduction in the combined height of lumbar vertebrae L3 and L4 (6,36 ±0,36mm vs 5,78 ±0,58mm; Figure 14F) of LRP4 ECD mutants as compared to controls. Furthermore, the inner and outer cortical perimeter of the femur mid-diaphyses was significantly smaller in LRP4 ECD mutants (Figure 14E, F, p<0,001 and p=0,002). These findings indicate that at least part of the reduction of the total body weight was due to impaired skeletal growth. Total femur bone mineral content (BMC) (Figure 14G) and bone mineral density (BMD) (Figure 14H) were also significantly reduced in LRP4 ECD mutants (BMC 11,1 ±1,3mg versus 9,0 ±1,5mg, p<0,05 and BMD 641,3 ±16,7mg/cc versus 602,3 ±21,4mg/cc, p<0,01).

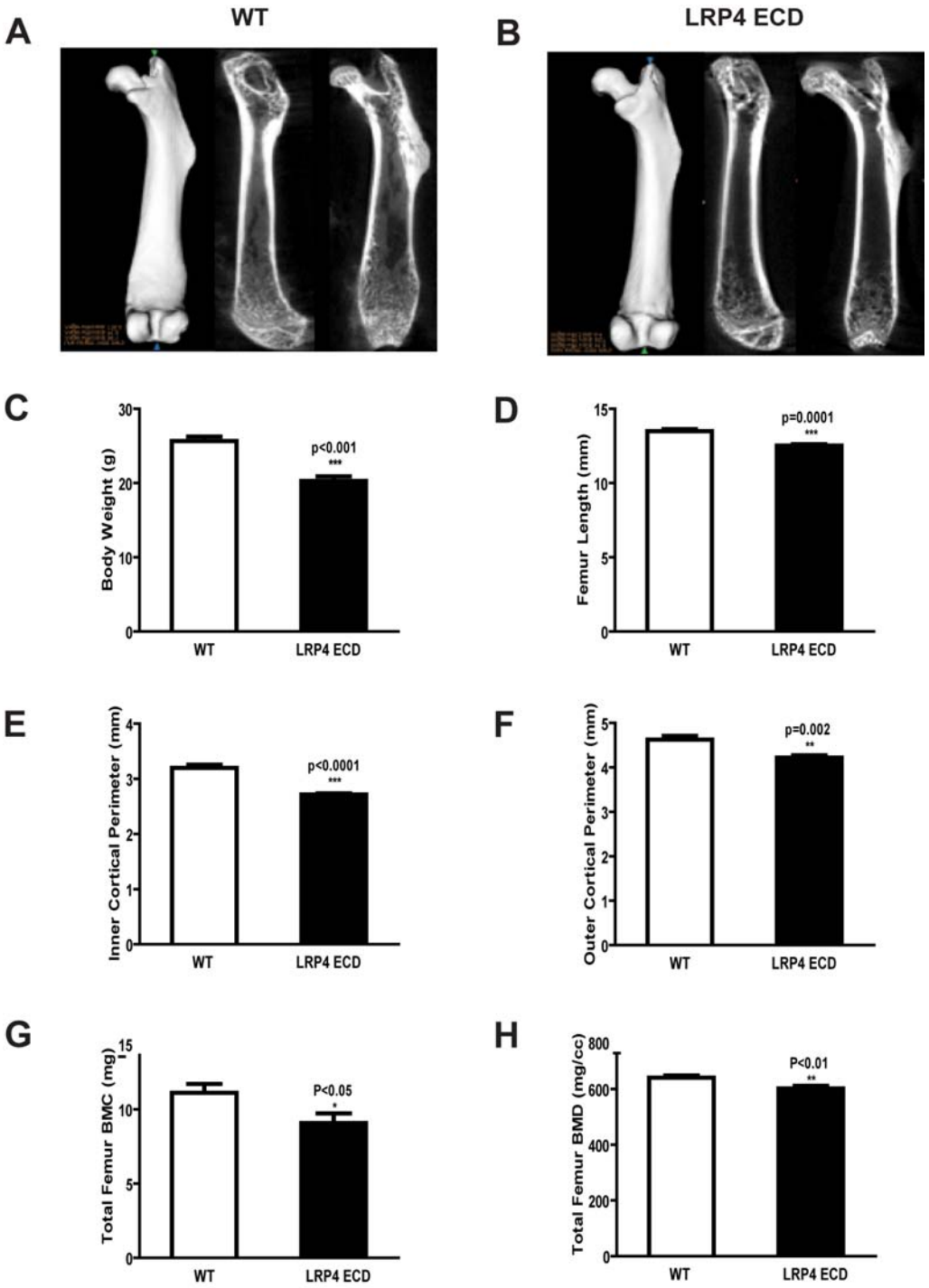

Figure 14 - Functional LRP4 deficiency results in impaired bone growth.

Representative μCT images of (**A**) wildtype (WT) and (**B**) low-density lipoprotein receptor related protein 4 (LRP4) extracellular domain (ECD) mouse femurs. (**C**) Total body weight of ten week old male mice was reduced in LRP4 ECD mice accompanied by a significant reduction of (**D**) femur length. Total (**E**) inner and (**F**) outer cortical perimeter of femur mid-diaphyses was significantly reduced in LRP4 ECD mice. Moreover, (**G**) total femur bone mineral content (BMC) and (**H**) bone mineral density (BMD) was significantly in LRP4 ECD mice. Calculations for the indicated parameters were performed using Microview software from GE Medical System. Results represent the average ±S.E. of values from six male mice.

To test whether reduced BMC and BMD are based on changes in cortical or trabecular bone, cortical femoral bone was scanned (Figure 15A, B). Interestingly, cortical thickness, cortical BMC and cortical BMD were unaffected (Figure 15C, D, E), suggesting that the difference in total femur BMD/ BMC was due to differences in the trabecular compartment of the femur.

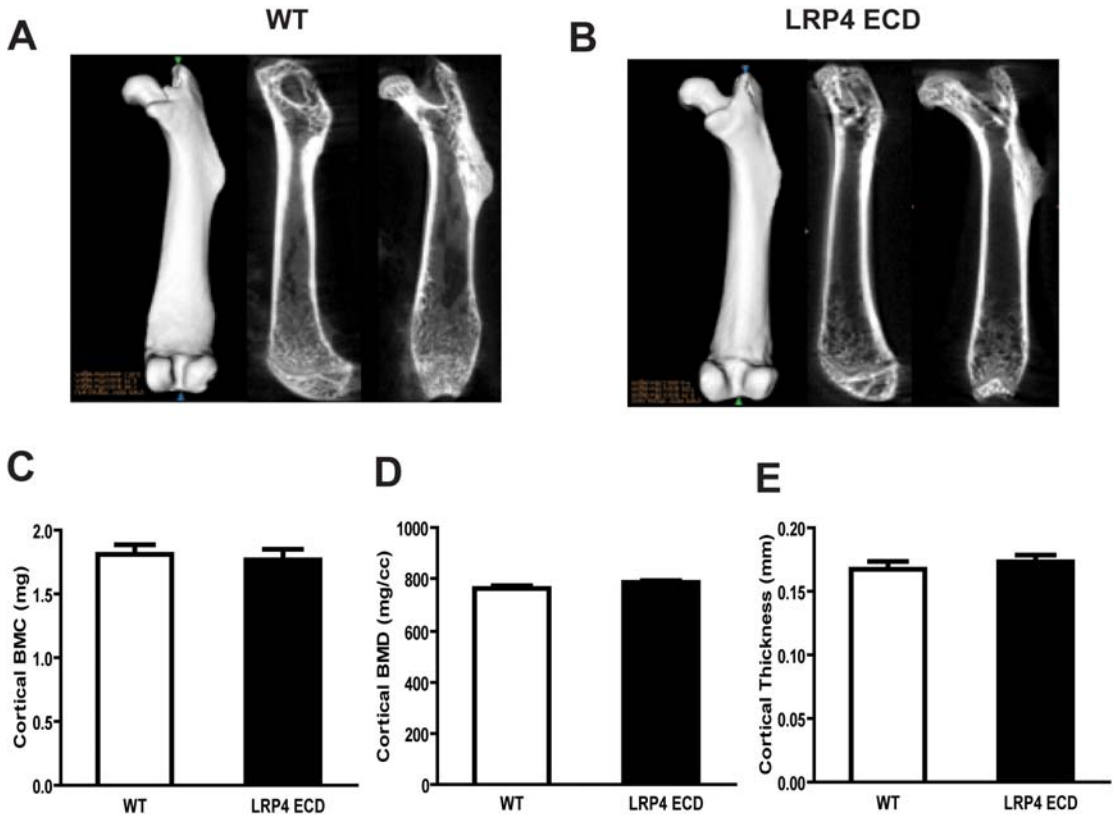

Figure 15 - Functional LRP4 deficiency does not alter cortical BMC, BMD, or thickness.
Representative µCT images of (**A**) wildtype (WT) and (**B**) low-density lipoprotein receptor related protein 4 (LRP4) extracellular domain (ECD) mouse femurs. **(C)** Cortical bone mineral content (BMC), (**D**) bone mineral density (BMD), and (**E**) cortical thickness were not altered in LRP4 ECD mice. Calculations for the indicated parameters were performed using Microview software from GE Medical System. Results represent the average ±S.E. of values from six male mice.

For the assessment of trabecular bone structure and density in mice, the lumbar spine is better suited than the distal femur or the proximal tibia. We therefore performed µCT on the lumbar vertebrae L3 and L4. Again, 3D and 2D reconstructions did not unveil gross abnormalities of lumbar spine morphology

(Figure 16A, B, F). However, trabecular bone analyses revealed a significantly reduced bone volume per total volume (BV/TV, 18,9 ±1,5% vs. 15,7 ±2,5%) in LRP4 ECD mutants as compared to wild type littermates (Figure 16C), accompanied by the according changes in trabecular separation and trabecular number (Figure 16D,E). Taken together, µCT analyses of the femur and lumbar spine indicate impaired bone growth in LRP4 ECD mutant mice, with smaller bones of otherwise mostly normal morphology and suggest a concomitant relative increase of bone resorption over bone formation, resulting in a net loss of trabecular bone.

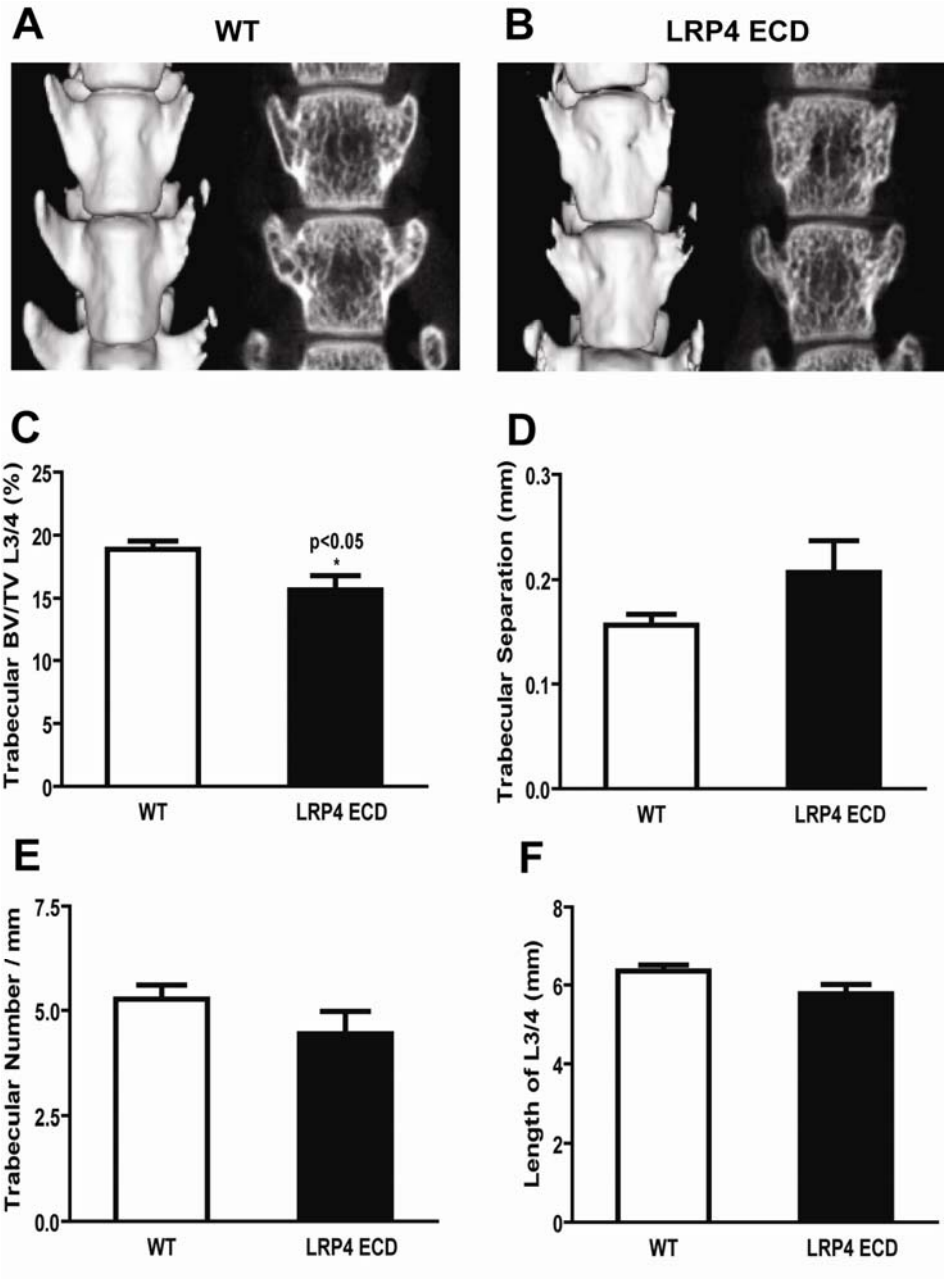

Figure 16 - Functional LRP4 deficiency results in reduced lumbar trabecular bone.
Representative µCT images of (**A**) wildtype (WT) and (**B**) low-density lipoprotein receptor related protein 4 (LRP4) extracellular domain (ECD) mouse lumbar vertebra L3 and L4. (**C**) Lumbar spine trabecular bone is significantly reduced in LRP4 ECD mice. In addition, a non-significant trend in (**D**) trabecular separation, (**E**) trabecular number per area, and (**F**) length of L3/4 indicates less trabecular bone in LRP4 ECD mice. Results represent the average±S.E. of values from six male mice.

3.1.4 Bone markers indicate increased bone turnover in LRP4 ECD mice

We also measured several biochemical markers that are indicative of bone turnover. Ten week old male animals were analyzed (n=14 per group) for the determination of turnover markers. Fasting blood and urine samples were obtained before sacrifice

according to a standardized time schedule to rule out any potentially confounding circadian alterations in the concentrations of the osteoblast activity markers alkaline phosphatase (ALP) and osteocalcin (OCN) as well as the urinary collagen breakdown product desoxypyridinoline (DPD) as a marker of osteoclast activity. We measured the osteoblast activity markers alkaline phosphatase (ALP, Figure 17A) and osteocalcin (OCN, Figure 17B) in serum. Both parameters were significantly elevated in the LRP4 ECD mutants (ALP: 230,2 ±22,3units/ml for WT and 365,5 ±41,1units/ml for LRP4 ECD littermates; OCN: 15,1 ±1,9ng/ml for WT and 22,0 ±3,9ng/ml for LRP4 ECD littermates), indicating increased bone formation in comparison to wild type control animals.

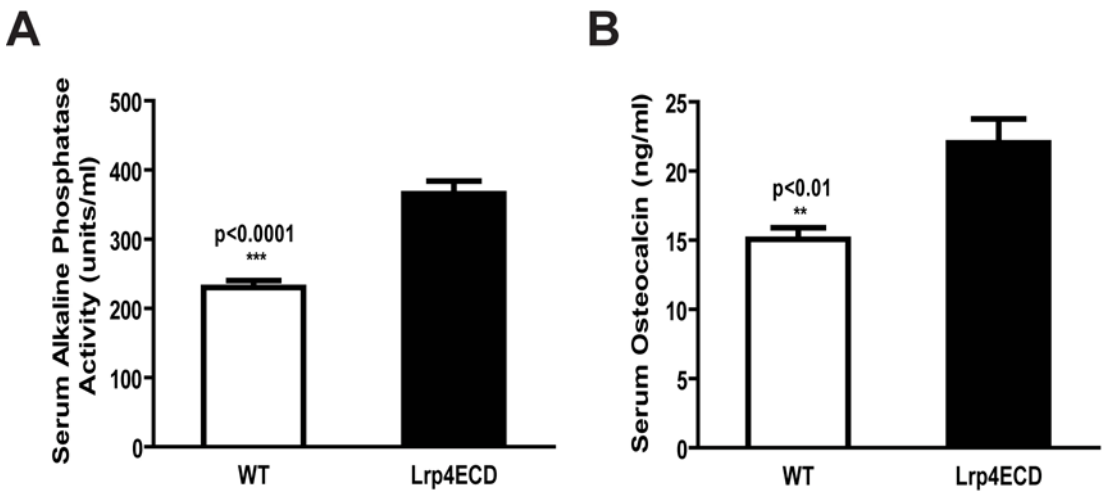

Figure 17 - Functional LRP4 deficiency results in increased bone formation markers ALP and OCN. Blood samples were collected from the same mice that were used for analyses in Figure 13 and 14. The bone formation markers (**A**) alkaline phosphatase (ALP) and (**B**) osteocalcin (OCN) are significantly increased in low-density lipoprotein receptor related protein 4 (LRP4) extracellular domain (ECD) mice (n=12 for both groups) indicating a higher bone formation rate.

To determine the osteoclast activity, urinary deoxypyridinoline (DPD) was measured and normalized against urinary creatinine levels (Figure 18). Increased DPD levels for LRP4 ECD mice (DPD/creatinine: 9,3 ±1,9nmol/mmol for WT and 11,4

±2,4nmol/mmol for LRP4 ECD littermates) suggests a higher bone resorption and overall higher bone turnover.

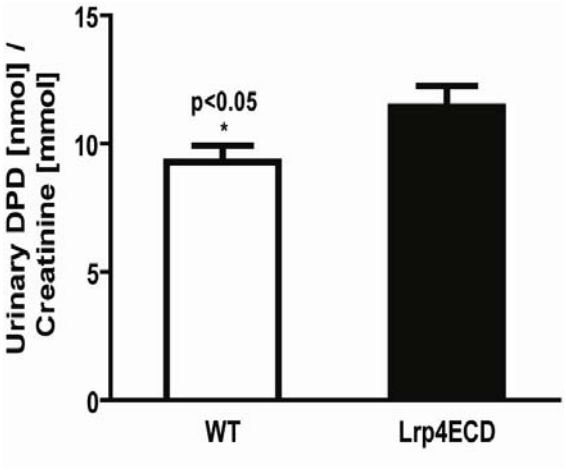

Figure 18 - Functional LRP4 deficiency results in increased bone resorption marker DPD/creatinine. Urine samples were collected from the same mice that were used for analyses in Figure 3 and 4. Urinary levels of DPD/creatinine are significantly increased in low-density lipoprotein receptor related protein 4 (LRP4) extracellular domain (ECD) mice (n=12 for both groups) indicating a higher bone resorption rate.

3.1.5 LRP4 deficiency does not alter osteoclastogenesis

Increased urinary DPD normalized against urinary creatinine levels suggest enhanced osteoclast activity and higher bone resorption. In order to further analyze osteoclast activity, osteoclastogenesis markers, e. g. cytokine RANKL and its decoy receptor OPG levels, were determined in serum. OPG RANKL levels were not significantly altered between groups both in males and females (OPG: wildtype: 426,7 ±16,90 for males and 336,4 ±22,00 for females; LRP4 ECD 455,40 ±30,73 for males and 375,2 ±25,62 for females; RANKL: wildtype: 51,06 ±7,87 for males and 66,36 ±5,32 for females; LRP4 ECD 65,50 ±8,02 for males and 71,64 ±8,00 for females) (Figure 19 A and D). Additionally, no effects could be shown for the ratio of OPG/RANKL levels (wildtype: 9,61 ±1,32 for males and 4,73 ±0,34 for females; LRP4 ECD 8,40 ±1,62 for males and 6,23 ±1,07 for females) suggesting no effect of functional LRP4 deficiency on osteoclastic differentiation.

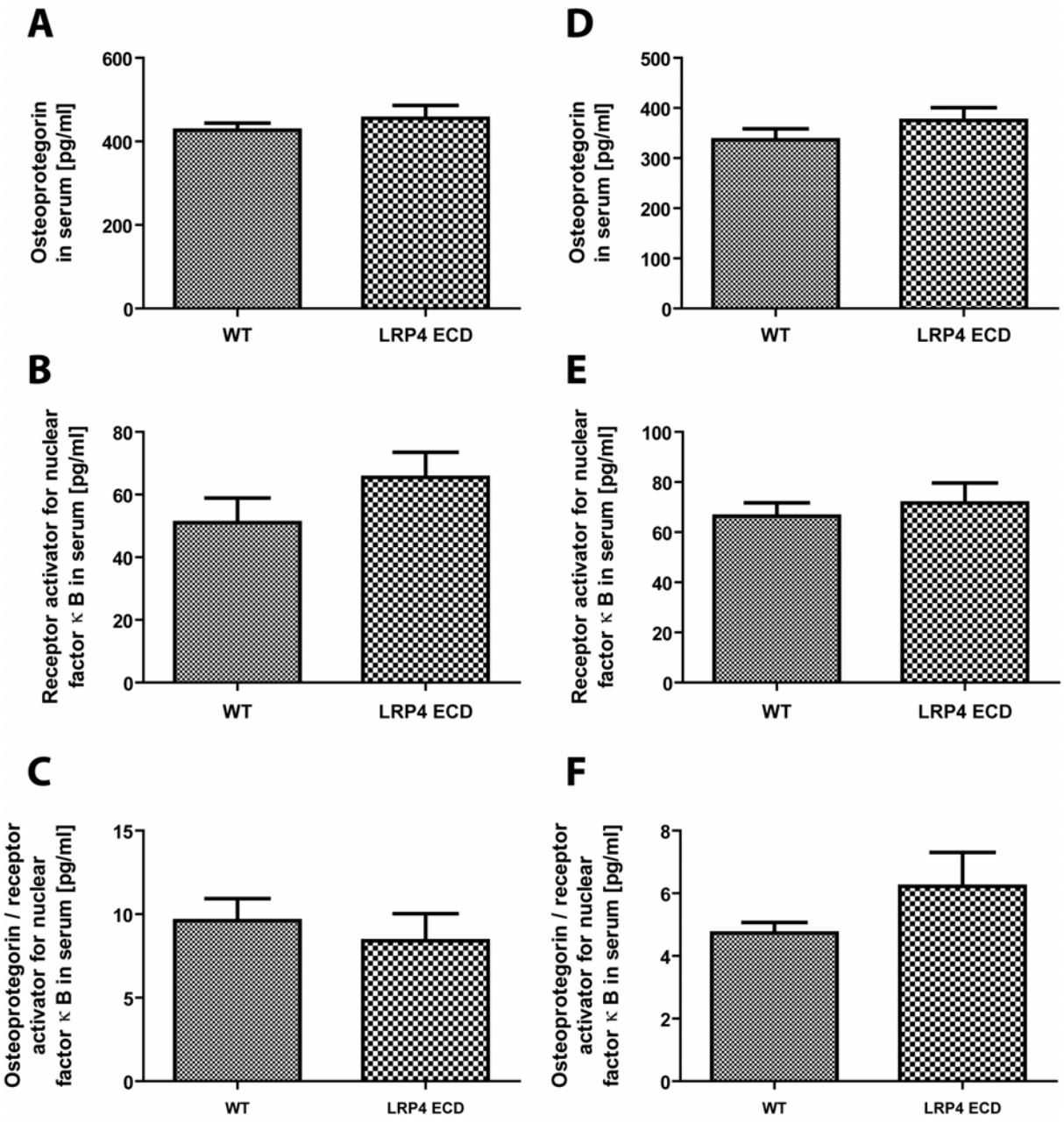

Figure 19 - Functional LRP4 deficiency does not alter osteoclastogenesis marker OPG/RANKL.

(**A, D**) Cytokine receptor activator for nuclear factor κ B ligand (RANKL), (**B, E**) decoy receptor osteoprotegorin (OPG), and the ratio of OPG to RANKL (**C, F**) in serum of 12 week old male (n=12 for both groups) (**A, B, C**) and female (n=12 for both groups) (**D, E, F**) mice. No significant differences could be shown for low-density lipoprotein receptor related protein 4 (LRP4) extracellular domain (ECD) mice compared to wildtype mice.

3.1.6 LRP4 deficiency results in decreased Wnt-signaling

To further explore the underlying cause of this phenotype, we analyzed the Wnt-signaling pathway in primary bone. Loss-of-function and gain-of-function of essential Wnt-signaling genes results in low bone mass and high bone mass phenotypes, respectively, indicating a crucial role in osteogenesis. Interestingly, LRP4 ECD mice show decreased levels of "activated" unphosphorylated β-catenin (Figure 20). The decreased levels of unphosphorylated β-catenin suggest a diminished Wnt-signaling in bone of LRP4 ECD mice.

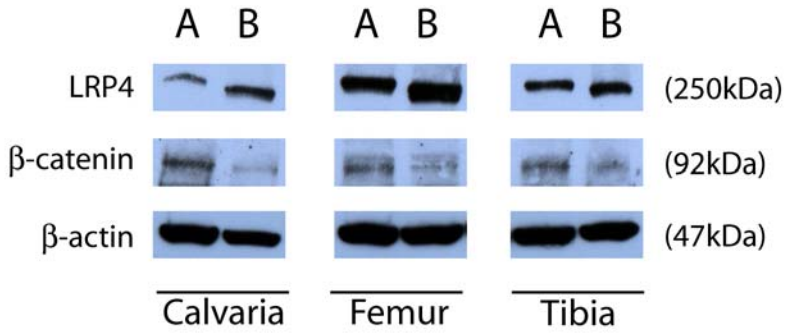

Figure 20 - Functional LRP4 deficiency results in reduced protein levels of unphosphorylated β-catenin.

Proteins were extracted from calvaria, femur, tibia as described in materials and methods and immunoblotted with specific LRP4 N-terminal, unphosphorylated β-catenin, and β-actin antibodies, respectively. Immunoblotting of unphosphorylated β-catenin revealed decreased levels in bone of (**B**) LRP4 ECD mice compared to (**A**) wildtype animals suggesting a diminished Wnt-signaling in bone of LRP4 ECD mice.

3.1.7 LRP4 deficiency does not alter RNA levels of Wnt target proteins

Dkk1 and SOST are highly potent Wnt-signaling inhibitors that bind to LRP5/6 and key regulator in bone metabolism. In addition we showed that these inhibitors physically interact with LRP4. To further analyse Wnt-signaling in bone we determined RNA expression levels of Wnt-signaling genes by quantitative RT-PCR measurements. Wnt-signaling inhibitor mRNA-levels Dkk1, Dkk2, and SOST are not significantly up or down-regulated in LRP 4 ECD mice compared to wildtype animals

(Figure 21A). Furthermore, no significant differences could be detected for mRNA expression levels of β-catenin and Wnt co-receptor LRP5/6 in LRP 4 ECD mice in comparison to wildtype animals (Figure 21B)

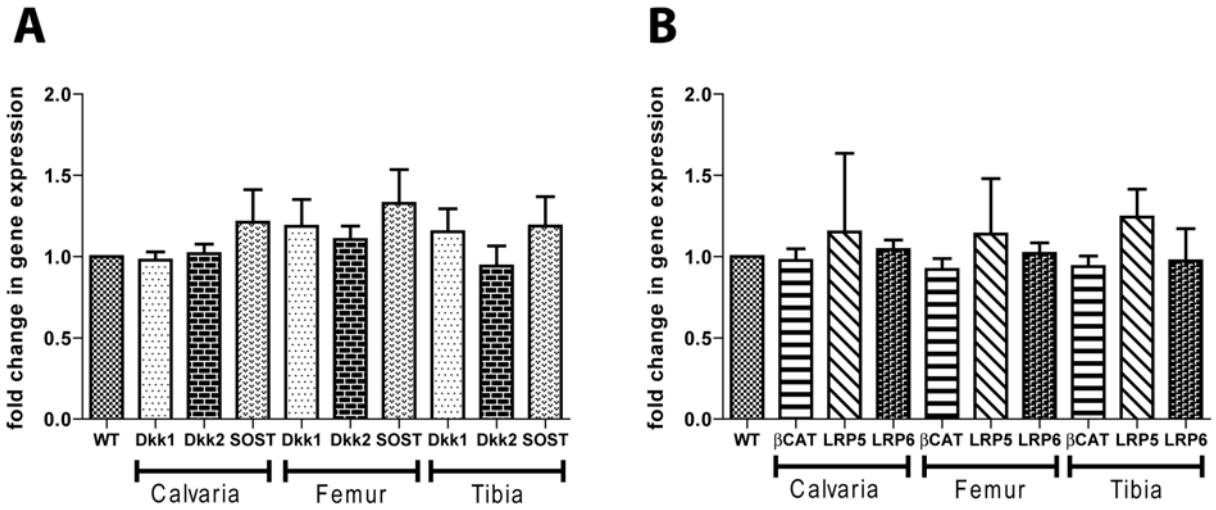

Figure 21 - RNA expression of Wnt-signaling genes in LRP4 ECD mice compared to WT mice
(**A**) RNA expression levels of Wnt-inhibitors Dickkopf 1 (Dkk1), Dickkopf 2, Dkk2, and Sclerostin (SOST) in calvaria, femur, and tibia in low-density lipoprotein receptor-related protein (LRP4) extracellular domain (ECD) mice compared to wildtype (WT) mice (n=4). (**B**) RNA expression levels of Wnt-signaling genes of β-catenin, LRP5 and 6 in calvaria, femur, and tibia in LRP4 ECD mice comparison to WT mice (n=4). No significant differences could be detected for the RNA expression of above mentioned genes in LRP4 ECD mice in comparison to wildtype mice.

3.2 Part 2 – ApoE in bone metabolism

3.2.1 Determination of correct genotype of specific ApoE isoforms

To determine the correct genotype, tissue samples of punched ears were digested with direct PCR tail (Viagen Biotech) to extract genomic DNA. Homozygosity of ApoE knockin allele was verified and DNA was extracted from the gel, cleaned up, and sequenced. Sequence analysis verified correct genotypes of mice used for biochemical and structural analysis (Figure 22A-C). Bodyweight of ApoE3 mice are significantly increased compared to ApoE2 mice (ApoE3: 19,58g ±0,42 compared to ApoE2: 21,62g ±0,36). No significant differences could be measured for ApoE4 mice (ApoE4 20,48g ±0,40), whose weight lies in between the bodyweight of ApoE2 and E3 animals (Figure 22D)

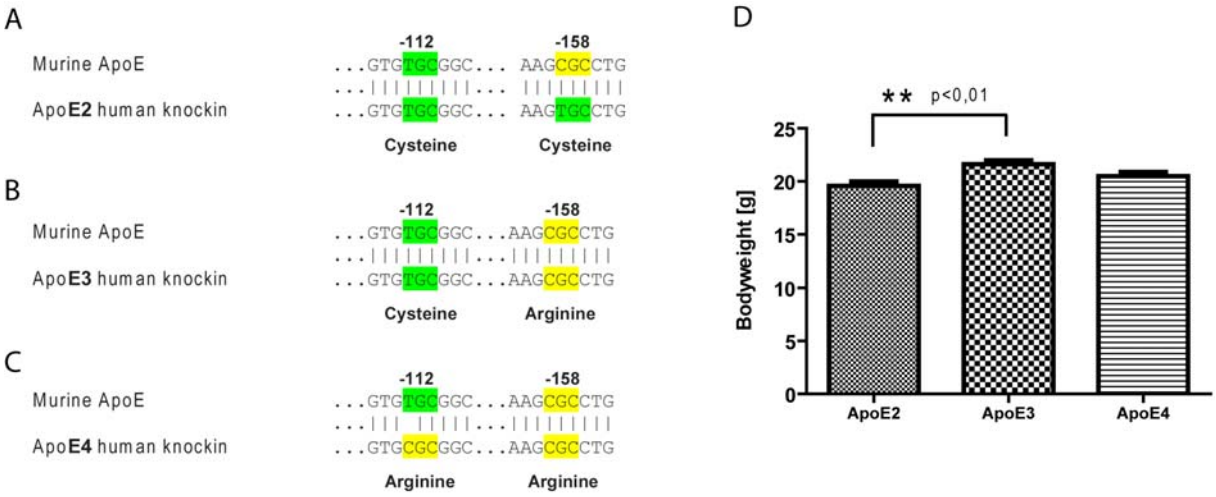

Figure 22 - Verification of correct genotype and bodyweight of human ApoE knockin mice.
(**A-C**) Illustration of sequencing analysis of ApoE mice carrying the human knockin ε2, ε3, and ε4 alleles. (**A**) Human ApoE2 carries a cysteine residue at positions 112 and 158, (**B**) human ApoE3 has a cysteine residue at position 112 and an arginine residue at position 158, and (**C**) human ApoE4 has an arginine residue at positions 112 and 158. (**D**) ApoE3 mice show a significantly higher bodyweight compared to ApoE2 mice, whereas the bodyweight of ApoE4 showed no significant differences to ApoE2 or E3 mice.

3.2.2 Bone formation markers are decreased in ApoE4 mice

To investigate bone metabolism we measured several biochemical markers that are indicative of bone turnover. Twelve week old female animals were analyzed (n=14 per respective genotype). Again, fasting blood and urine samples were obtained to a standardized time schedule to rule out any potentially confounding circadian alterations. We measured the osteoblast activity markers alkaline phosphatase (ALP) and osteocalcin (OCN) in serum. For the more unspecific bone formation marker ALP, a significant difference could be detected between ApoE3 and ApoE4 animals, whereas ApoE2 mice did not show any significant differences to the other groups (ALP: ApoE2: 458,3 ±25,04 SigmaUnits/ml; ApoE3 484,2 ±21,43 SigmaUnits/ml; ApoE4 409,8 ±17,38 SigmaUnits/ml) (Figure 23A). For the more specific bone marker OCN, serum levels of ApoE2 and ApoE3 mice are significantly higher than ApoE4 indicating increased bone formation for these animals in comparison to ApoE4 (OCN: ApoE2: 21,17ng/ml ±0,85; ApoE3 21,16ng/ml ±0,42; ApoE4 19,08ng/ml ±0,48, Figure 23B).

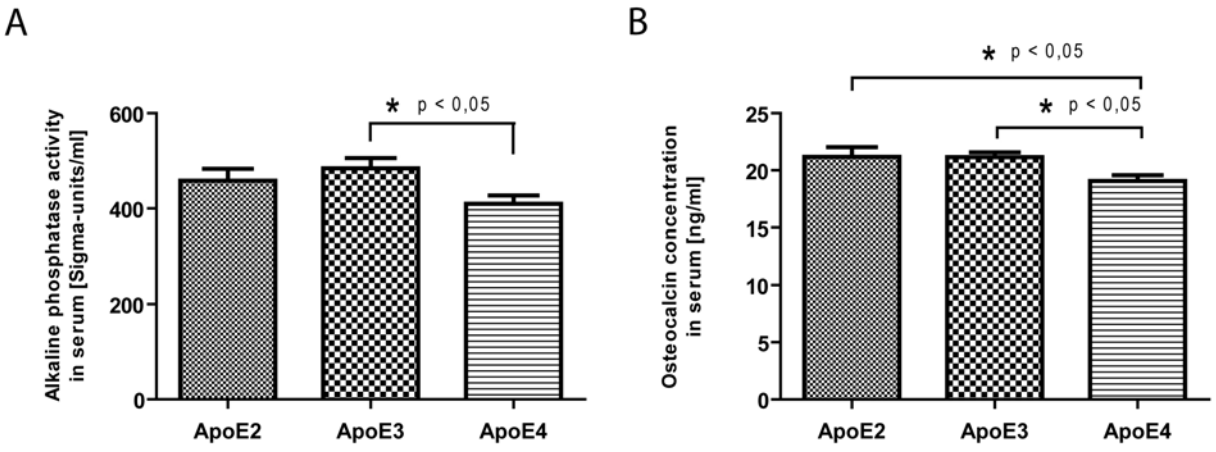

Figure 23 - Serum bone formation markers ALP and OCN are reduced in ApoE4 mice.
(**A**) Bone formation markers alkaline phosphatase (ALP) and (**B**) osteocalcin (OCN) in serum of 12 week old ApoE2, E3, and E4 mice. Data are means ± S.E.M. for above mentioned biochemical bone formation markers in serum of ApoE2 (n = 14), E3 (n =14), and E4 (n = 14) mice. Serum osteocalcin levels were significantly reduced in ApoE4 mice compared to ApoE3 and ApoE2 animals.

3.2.3 Bone resorption marker DPD is increased in ApoE2 mice

To determine the osteoclast activity, urinary bone breakdown product deoxypyridinoline (DPD) was measured and normalized against respective urinary creatinine levels (Figure 24). Statistical analysis revealed significantly enhanced DPD levels for ApoE2 mice compared to ApoE4 animals and a statistical trend towards ApoE3 mice. No differences could be measured between ApoE3 and ApoE4 animals (Figure 24)

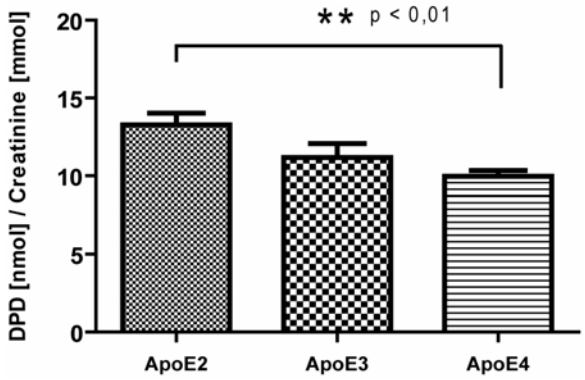

Figure 24 - Urinary bone resorption marker DPD/creatinine is increased in ApoE2 mice.
Bone resoption marker deoxypyridinoline (DPD) in unrine of 12 week old ApoE2, E3, and E4 mice normalized against respective urinary creatinine levels. Data are means ± S.E.M. for above mentioned biochemical bone resorption marker in urine of ApoE2 (n = 14), E3 (n =14), and E4 (n = 14) mice. Urinary DPD/creatinine is significantly increased in ApoE2 mice compared to ApoE3 and E4 animals.

3.2.4 Osteoclastogenesis marker OPG/RANKL ratio indicates increased osteoclastic differentiation in ApoE2 mice

Osteoclastogenesis is primarily regulated by the cytokine RANKL and its decoy receptor OPG. To further investigate the high osteoclastic activity in ApoE2 mice, we measured these osteoclastic markers in serum. RANKL levels are significantly increased in ApoE2 mice compared to ApoE3 and E4 animals. (RANKL: ApoE2: 136,1pg/ml ±9,01; ApoE3 99,33pg/ml ±6,61; ApoE4 82,44pg/ml ±3,97 (Figure 25A). OPG decoy receptor levels are significantly decreased in ApoE4 compared to

ApoE2 and E3 mice (OPG: ApoE2: 501,6pg/ml ±24,22; ApoE3 537,3pg/ml ±29,01; ApoE4 432,6pg/ml ±16,02 (Figure 25B). The OPG/RANKL ratio is a critical regulator of bone metabolism; therefore an imbalanced of OPG to RANKL ratio suggests an impaired functional balance between osteoblasts and osteoclasts. However, the OPG/RANKL ratio is significantly decreased in ApoE2 mice compared to ApoE3 and E4 animals (OPG/RANKL ratio: ApoE2: 3,58pg/ml/pg/ml ±0,17; ApoE3 5,62pg/ml/pg/ml ±0,47; ApoE4 5,50pg/ml/pg/ml ±0,38 (Figure 25C) suggesting induced osteoclastic differentiation in ApoE2 mice, which is consistent with increased osteoclastic activity in these animals.

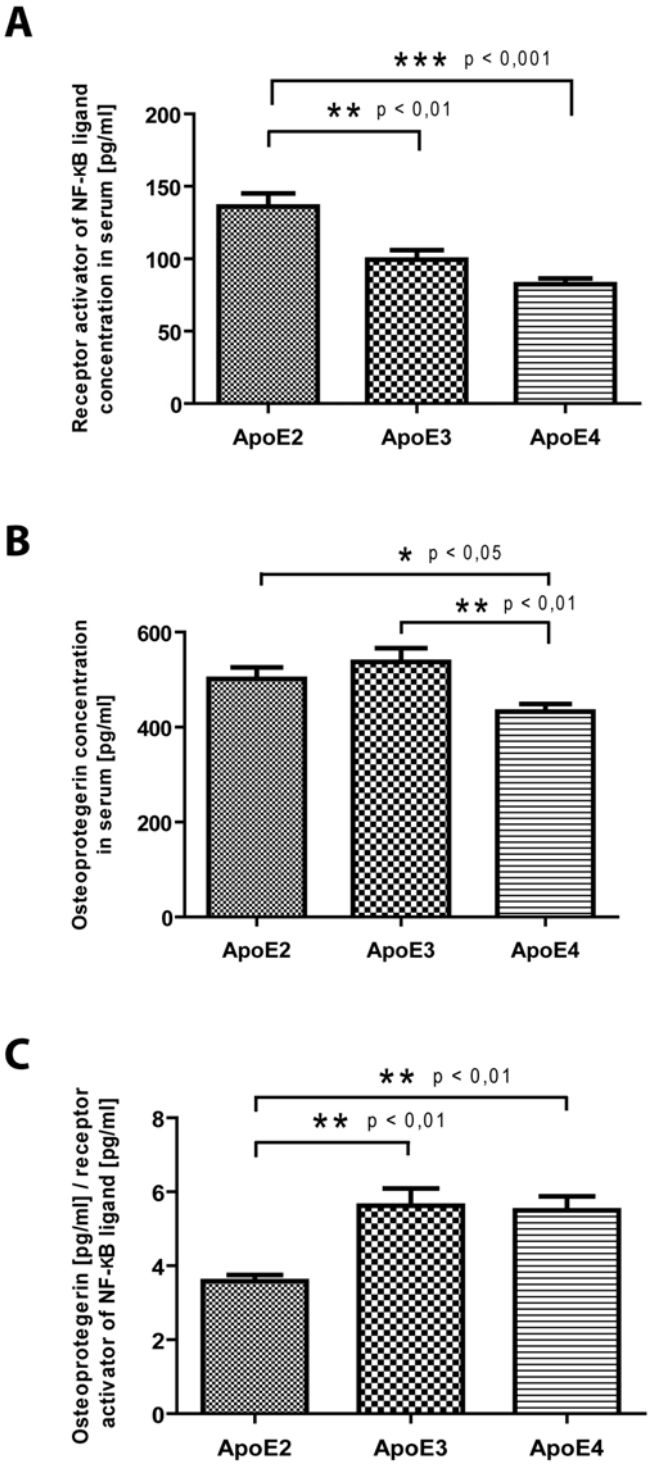

Figure 25 - Serum bone osteoclastogenesis marker ratio OPG/RANKL is reduced in ApoE2 mice.
Cytokine receptor activator for nuclear factor κ B ligand (RANKL) (**A**), decoy receptor osteoprotegorin (OPG) (**B**), and the ratio of OPG to RANKL (**C**) in serum of 12 week old ApoE2, E3, and E4 mice. Data are means ± S.E.M. for above mentioned biochemical bone formation markers in serum of ApoE2 (n = 14), E3 (n = 14), and E4 (n = 14) mice. Serum RANKL levels are significantly increased in ApoE2 mice compared to ApoE3 and E4 animals whereas OPG levels were significantly in ApoE2 and E3 mice in comparison to ApoE4 animals. OPG/RANKL ratio display a significant reduced ratio for ApoE2 compared to ApoE3 and E4 animals.

3.2.5 ApoE2 results in reduced trabecular bone volume in femoral bone

To investigate the physiological consequence of the above shown findings of bone formation, bone resorption, and osteoclastogenesis marker for the respective ApoE isoforms on bone metabolism, we performed µCT analysis of femoral bone on 13 week old female mice (n=8 per group). This analysis revealed significantly increased cortical bone thickness for ApoE3 mice compared to ApoE4 animals. No significantly altered thickness could be detected for ApoE2 mice in comparison to the other groups (ApoE2 0,1919 ±0,0031; ApoE3 0,1957 ±0,0021; ApoE4 0,1957 ±0,0021) (Figure 26A). Femoral bone volume/total volume (BV/TV) of trabecular bone is significantly increased in ApoE3 compared to ApoE2 animals and ApoE4 animals. Furthermore, ApoE4 mice display significantly increased femoral bone volume/total volume of trabecular bone in comparison to ApoE2 animals (ApoE2 3,92 ±0,52; ApoE3 6,27 ±0,30; ApoE4 5,14 ±0,251) (Figure 26B).

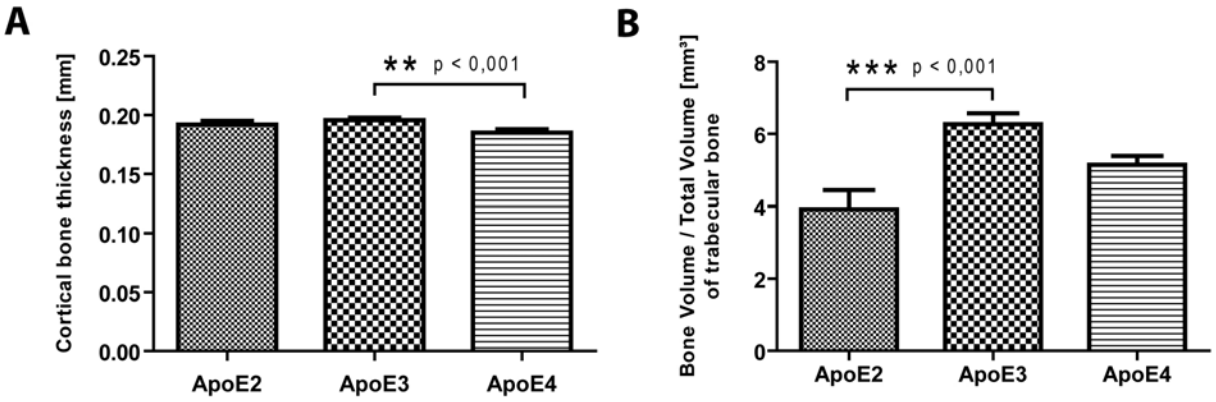

Figure 26 - ApoE2 isoform results in reduced trabecular bone volume in femoral bone.
(**A**) µCT scans of femoral bone of ApoE2, E3, and E4 mice (n=8 per group) revealed a significantly increased cortical bone thickness for ApoE3 mice compared to ApoE4 animals. (**B**) In addition, bone volume/total volume of trabecular bone is significantly increased in ApoE3 mice in comparison to ApoE2 and ApoE3 animals.

3.2.6 ApoE2 results in reduced bone quality and stability

In order to test the consequences of varying bone turn over and osteoclastogenesis markers, and trabecular bone architecture for the respective ApoE isoforms on biomechanical stability, we conducted a three-point bending assay. Biomechanical analysis of femoral bone revealed significantly reduced biomechanical stability for ApoE2 and ApoE4 mice compared to ApoE3 animals (ApoE2 17,48 F_{max} ±0,55; ApoE3 19,69 F_{max} ±0,66; ApoE4 17,51 F_{max} ±0,28) (Figure 27A). Interestingly, tested femoral bone displayed significantly lowered energy absorbance in an isoform-specific manner (ApoE2 3,12 F_{max} * mm ±0,24 < ApoE3 4,01 F_{max} * mm ±0,25 <ApoE4 5,74 F_{max} * mm ±0,58) (Figure 27B).

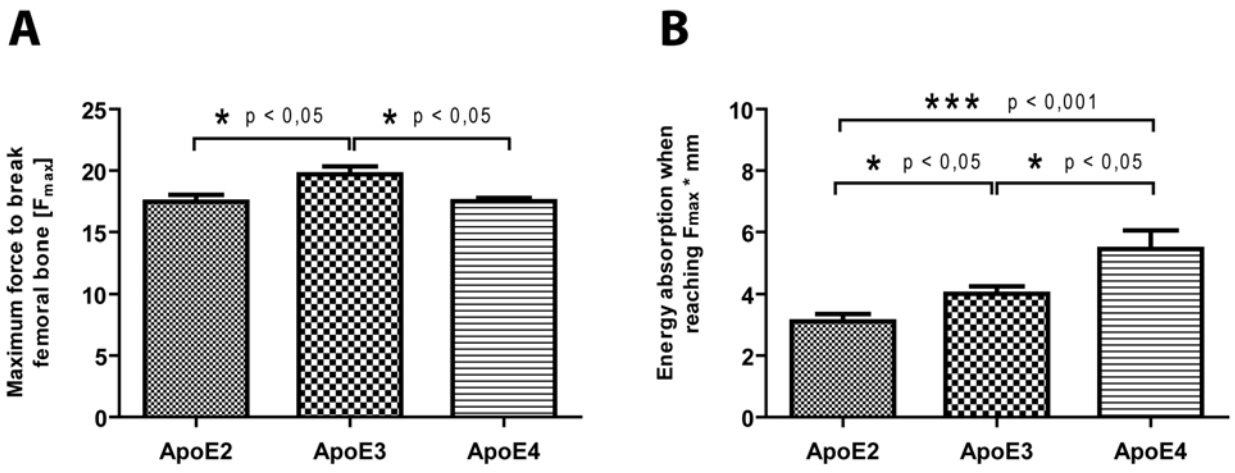

Figure 27 - ApoE2 isoform causes reduced biomechanical stability in femoral bone.
(**A**) Three point binding assay revealed a significantly reduced biomechanical stability (force to failure) in ApoE2 and ApoE4 mice compared to ApoE3 animals (n=8 per group). In contrast, the energy absorbance of femoral bone significantly increases in an ApoE-specific manner (ApoE2<ApoE3<ApoE4; n=8 per group).

3.2.7 ApoE2 results in reduced bone volume in lumbar spine

To further assess reduced trabecular bone in human ApoE knockin mice, we performed histological analysis on lumbar vertebrae L4 in these mice. For the precise assessment of trabecular bone structure and density in mice, the lumbar

spine is a better suited location than the distal femur. For comparative quantitative histomorphometry, the undecalcified lumbar spines were stained and measured using Osteometrix in a blinded fashion. Analysis revealed significantly reduced BV/TV of trabecular bone in lumbar vertebrae in ApoE2 mice compared to ApoE3 and ApoE4 animals (Figure 28A and B). This effect is accompanied by significant differences in trabecular number (Figure 28C), trabecular thickness (Figure 28D). The same pattern between groups is observed for trabecular separation whereas significant differences could be observed between ApoE2 and ApoE4 mice only (Figure 28E).

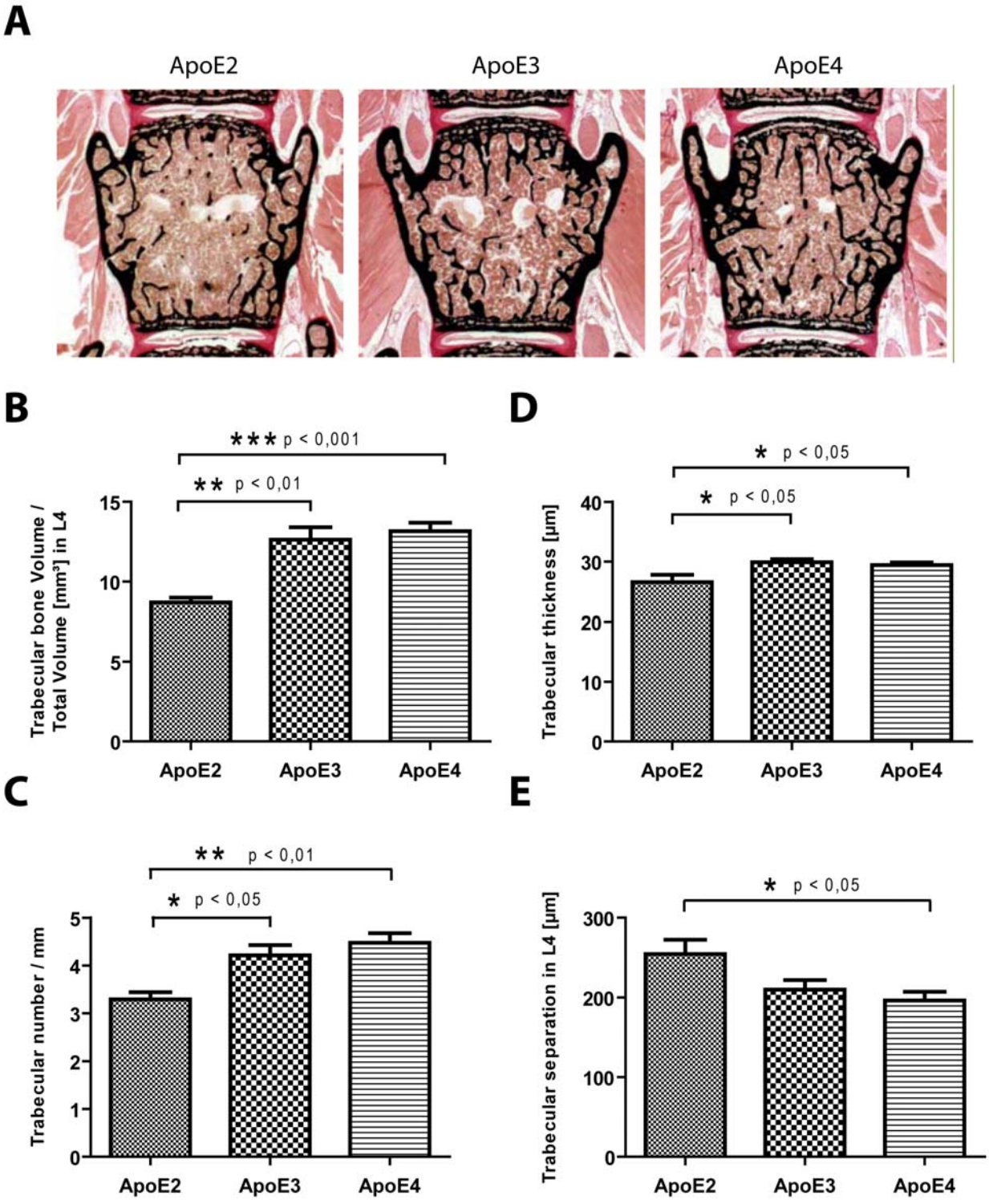

Figure 28 - ApoE2 isoform results in reduced trabecular bone in lumbar vertebra L4.

(**A**) Representative histological images of respective ApoE isoform lumbar vertebrae L4. (**B**) histological analysis of lumbar vertebrae L4 revealed significantly reduced bone volume/total volume of trabecular bone in ApoE2 mice compared to ApoE3 and ApoE4 animals (n=8 per group). In addition, significant differences in (**C**) trabecular number, (**D**) trabecular thickness, and (**E**) trabecular separation in L4 indicates less trabecular bone in ApoE2 mice compared to ApoE3 and ApoE4 animals could be determined.

3.2.8 ApoE2 isoform results in decreased bone formation

To further determine whether the low bone-mass phenotype of ApoE2 human knockin mice is caused by decreased bone formation or increased bone resorption, we assessed bone formation in vivo by fluorochrome measurements of mice injected twice with calcein label as described in materials and methods. Representative fluorescent micrographs show a significant decrease in bone formation for ApoE2 animals compared to ApoE3 and ApoE4 animals (Figure 30A/B) indicating a lower osteoblastic activity and lower bone formation for these animals *in vivo*.

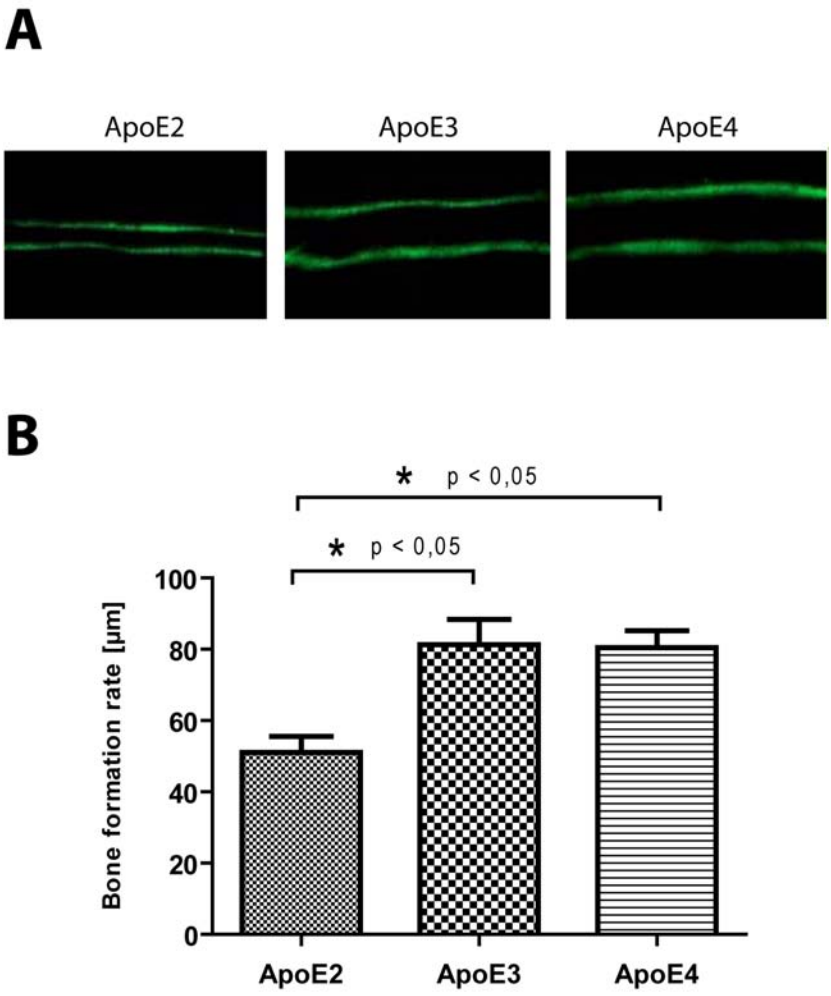

Figure 29 - ApoE2 isoform results in reduced bone formation *in vivo*.

(**A**) Representative fluorescent micrographs display the two calcein-labeled mineralization fronts with the distance between them indicating osteoblast functional activity of respective human ApoE knockin mice. (**B**) ApoE2 mice show a significant reduction in bone formation compared to ApoE3 and ApoE4 animals (n=5 per group).

4. Discussion

4.1 Part 1 – LRP4 in bone metabolism

LRP4, member of the LDLR family, is a multifunctional membrane-bound receptor that is important for the proper development and morphogenesis of limbs, ectodermal organs, lungs and kidneys. Moreover, this receptor is essential for the formation of postsynaptic neuromuscular junctions (Weatherbee et al. 2006). The structural organization of the extracellular domain of LRP4 closely resembles that of LRP5/6, two members of a subgroup of LRPs that function as co-receptors in the Wnt-signaling cascade (Tamai et al. 2000). LRP4 is important for control and modification of Wnt-signaling by its suggested antagonistic on canonical Wnt-signaling, a pathway which is crucial in bone metabolism. It is thought to be mediated in part by a displacement of the homologous LRP5/6 proteins in the co-receptor complex formed by Fz with LRP5/6, which is required to bind Wnt proteins and to transduce the Wnt signal to downstream elements of the canonical cascade (Li et al. 2010). Interestingly, in collaborative large-scale meta-analysis of genome-wide association studies, LRP4 has been associated with lumbar spine and femoral neck BMD highlighting the crucial impact of this receptor to variation in BMD (Rivadeneira et al. 2009; Richards et al. 2009).

Here we report that LRP4 is expressed by murine bone, specifically by osteoblasts, and binds the two secreted Wnt modulators Dkk1 and SOST. Furthermore, mice carrying a hypomorph mutation in LRP4 (LRP4 ECD) have impaired bone growth and increased bone turnover. Protein-analysis of activated β-catenin (unphosphorylated β-catenin) revealed lower levels of unphosphorylated β-catenin in three different locations (calvaria, femur, and tibia) of primary bone samples in LRP4 ECD mice suggesting diminished Wnt/β-catenin-signaling in these

mice. However, RT-PCR measurements did not reveal any altered RNA expression levels for Wnt-signaling genes, e. g. β-catenin, LRP5, LRP6 etc., in mice with functional LRP4 deficiency.

The Wntβ-catenin-signaling is of crucial importance for osteogenesis and has probably been the most intensely studied signaling pathway in bone in recent years. LRP5 and LRP6 have been recognized as the main osteoblast expressed co-receptors of the frizzled family of proteins, which together form a receptor complex at the cell surface that binds the Wnt-signaling proteins and thereby initiates the canonical signaling cascade. The finding that LRP4 is also expressed by osteoblasts in bone has important implications for the understanding of the complexity of the regulation of the canonical Wnt-signaling pathway in bone. SOST and Dkk1 are effective inhibitory modulators of the Wnt/β-catenin-pathway and it has been generally assumed that these molecules exert their antagonistic effect mainly through direct binding to LRP5/6, thereby blocking binding sites on these receptors for the pathway activating Wnts. Interestingly, Wnt/β-catenin-pathway inhibitor SOST has been associated with lumbar spine and femoral neck BMD (Rivadeneira et al. 2009; Richards et al. 2009). Here we have shown that LRP4 efficiently binds both SOST and Dkk1, suggesting that at the osteoblast surface, LRP4 may compete with LRP5/6 for the interaction with SOST and Dkk1. LRP4, but not LRP5/6, contains an NPXY endocytosis motif in its cytoplasmic domain. However, it is not known whether LRP4 contributes to the endocytosis of extracellular molecules to a significant extent. The exact nature of both the cellular consequences of SOST and Dkk1 binding to LRP4 will be determined by future studies. However, functional LRP4 deficiency does not alter RNA expression levels neither of Wnt-signaling inhibitors SOST or Dkk1/2 nor of Wnt-signaling genes like LRP5/6, β-catenin.

How can we bring the new interaction of LRP4 with Wnt/β-catenin-signaling inhibitors Dkk1 and SOST in context with reduced bone in LRP4 ECD mice? Recently, Ohazama and colleagues showed that LRP4 integrates BMP and Wnt signals in tooth development in mice (Ohazama et al. 2008) by binding Wise, a secreted BMP antagonist that also binds to LRP6 and thereby inhibits Wnt-signaling. In analogy to Wise, SOST and Dkk1 are two other LRP5/6 ligands that we have now shown to also interact with LRP4. Besides the proposed function of LRP4 as a negative modulator, one possible mechanism is that LRP4 simply acts as a sink and competes with LRP5/6 for the binding of these Wnt antagonists, which then are no longer available for suppression of the signal through the LRP5/6 axis. The reduced levels of "activated" unphosphorylated β-catenin we detected in different locations in bone of LRP4 ECD mutant mice in comparison to wildtype animals, could be a direct result of the increased availability of extracellular Wnt-antagonists, leading to a net inhibitory effect on canonical Wnt/β-catenin-signaling in bone. This novel function of LRP4 and its effect on the Wnt/β-catenin-signaling pathway would provide an explanation for the reduced lumbar spine trabecular BV/TV in the LRP4 ECD mutant mice. Furthermore, both Wnt-signaling and BMP-signaling are involved in the growth plate organization and enchondral ossification process (Kobayashi et al. 2005; Chen et al. 2008; Perry et al. 2008). LRP4 can by itself inhibit Wnt-signaling, presumably by competing for LRP5/6 in the Wnt/Fz complex (Johnson et al. 2005). Since SOST can inhibit BMPs, and Dkk1 is itself regulated by BMPs, it is likely that the failure to properly integrate BMP and Wnt-signaling pathways in the absence of a normal, functional LRP4 is responsible for the reduced limb length growth in the LRP4 ECD mutants. Such a mechanism would be analogous to the role of LRP1 in the integration of PDGF and TGFβ signals in the vascular wall, where loss of LRP1 expression in smooth muscle cells results in the simultaneous deregulation of PDGF

as well as TGFβ signalling with medial hypertrophy, elastolysis and fibrosis (Boucher et al. 2003/2007; Zhou et al. 2009).

The elevated concentration of biochemical bone turnover markers, serum osteocalcin, alkaline phosphatase and urinary DPD in LRP4 ECD animals indicate that both osteoblast and osteoclast activities are significantly increased in these mice. The enhanced osteoblastic function cannot be explained by altered Wnt/β-catenin-signaling since protein levels of "activated" unphosphorylated β-catenin are decreased in LRP4 ECD mice and therefore must be Wnt/β-catenin-signaling independent. Osteoblast-specific changes in Wnt- and BMP-signaling controls osteoclast differentiation based on altered expression of OPG (Glass et al. 2006). Serum OPG/RANKL levels were not affected in LRP4 ECD mice suggesting an osteoblast-independent mechanism responsible for the increased osteoclastic function.

4.1.1 Part 1 - conclusions

In conclusion, the expression of LRP4 by osteoblasts, its novel interaction with Wnt-signaling inhibitors Dkk1 and SOST, and the lower levels of activated β-catenin in three different bone locations described here, adds another player to the long list of established factors that modulate canonical Wnt-signaling in bone. By demonstrating that in addition to Wise, LRP4 is able to interact with two additional important modulators of Wnt- and BMP-signaling, our perspective of the complexity of the integration of BMP and Wnt-signaling pathways on the osteoblast surface has expanded further. Nevertheless the recently described association of both the SOST and LRP4 genes with BMD in humans, together with our findings suggest that LRP4 plays a physiologically important role in the skeletal development and bone metabolism not only in rodents, but in humans as well. The efficiency with which

LRP4 binds both SOST and Dkk1, presumably at the osteoblastic surface, LRP4 could simply act as a sink and competes with LRP5/6 for the binding of these Wnt antagonists, which then are no longer available for suppression of the signal through the LRP5/6 axis (Figure 31).

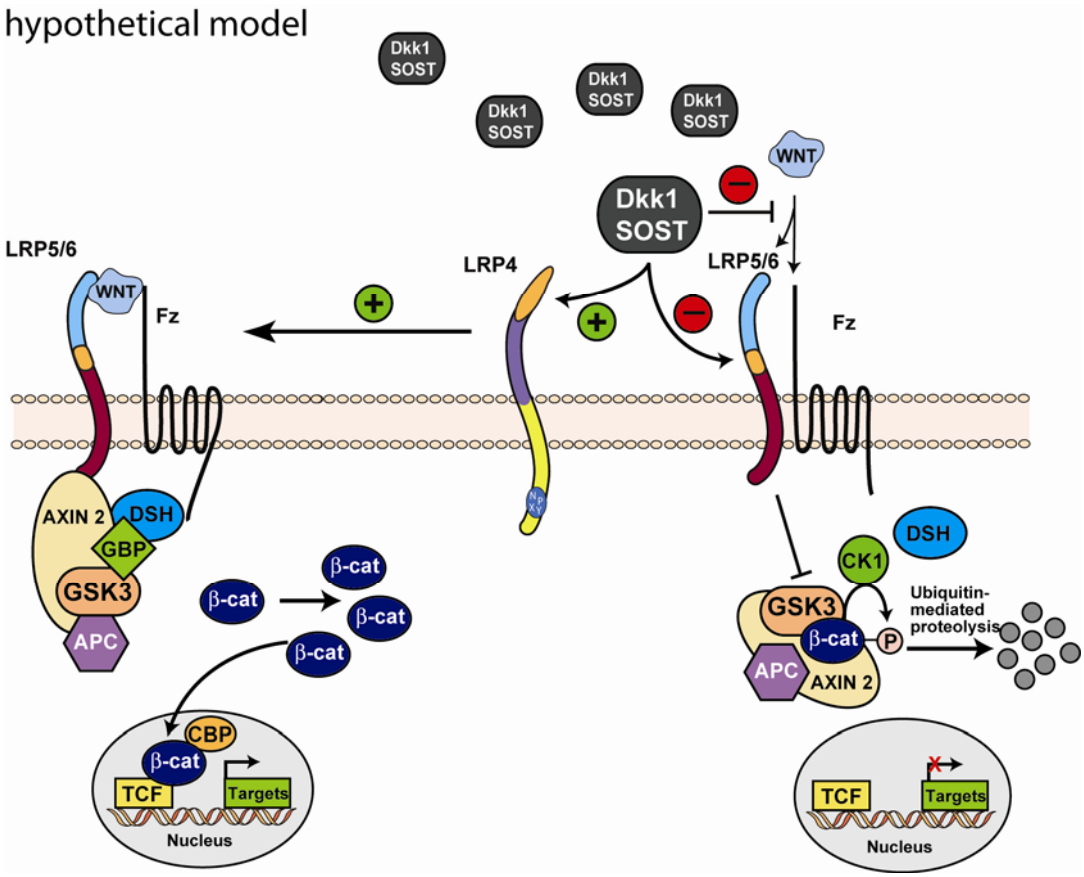

Figure 30 – Hypothetical model for the effect of LRP4 in bone.
Wnt-signaling inhibitors Dkk1 and SOST bind Wnt co-receptors LRP5/6 and block canonical Wnt-signaling which results in the phosphorylation of β-catenin and subsequent proteasomal degradation. LRP4 may act as a sink for Dkk1 and SOST and compete with LRP5/6 for the binding of these Wnt antagonists, which then are no longer available for suppression of the signal through the LRP5/6 axis resulting in the accumulation of "activated" unhosphorylated β-catenin that translocates to the nucleus and regulates gene expression.

4.1.2 Part 1 – outlook

The current study cannot distinguish whether the observed bone phenotype of the LRP4 ECD mutant is due to an impaired interaction of osteoblast expressed LRP4 with Dkk1, with SOST, or most likely with both proteins. Future studies will address to what degree the phenotype is synthetic, e.g. by analyzing mice with osteoblast-specific inactivation of LRP4 in combination with mutations in Dkk1 and SOST.

The Wntβ-catenin-signaling is of crucial importance for osteogenesis and has probably been the most intensely studied signaling pathway in bone in recent years. The finding of decreased “activated” β-catenin protein levels in different bone locations in LRP4 ECD mice suggests for the first time an impaired Wnt/β-catenin-signaling in mice with functional deficient LRP4. Extensive further studies in primary osteoblastic, osteoclastic, and osteocytic cell lines are clearly necessary to fully understand the mechanisms by which LRP4 deficiency leads to impaired Wnt/β-catenin-signaling in LRP4 ECD mice.

4.2 Part 2 – ApoE in bone metabolism

ApoE, a 299 amino acid glycoprotein, is a crucial regulator in the uptake of triglyceride, phospholipids, cholesteryl esters, and cholesterol into cells (Eichner et al. 2002). Thus, ApoE plays a protective role in the pathogenesis of atherosclerosis by preventing high cholesterol levels in plasma (Curtiss et al. 2000). Isoelectric focusing-based studies have revealed three main isoforms of ApoE in humans (Mahley et al. 1988) with single amino-acid substitutions at position 112 and 158 (Martins et al. 1995). ApoE3 (ε3) contains cysteine and arginine, respectively, whereas ApoE2 (ε2) has two cysteines and ApoE4 (ε4) has two arginines at these positions (Weisgraber et al. 1981). ApoE3 and E4 bind to LDL receptors with similarly high affinity, whereas the binding of ApoE2 is 50 to 100 times weaker (Weisgraber et al. 1982). In this context ApoE2 is associated with type III hyperlipoproteinemia (Mahley et al. 2001).

Here we report that human ApoE knockin mice display diverse effects for respective ApoE isoforms on bone metabolism. ApoE2 mice show decreased trabecular bone volume per total volume in femoral bone and lumbar spine in comparison to ApoE3 and E4 animals. In this context, urinary bone resorption marker DPD is increased in these animals, which is accompanied by a low ratio of osteoclastogenesis markers OPG/RANKL. Interestingly, serum bone formation markers ALP and OCN are diminished in ApoE4 mice. In contrast to this finding, ApoE2 show the lowest bone formation rate compared to other groups *in vivo*.

Bone metabolism has long been studied from a perspective that did not recognize the potential importance of systemic metabolic processes, such as lipid metabolism. Recent experimental data shows that CR are delivered to bone cells *in vivo*, accounting for almost 20% of liver uptake (Niemeier et al. 2008). Growing experimental evidence suggests that lipid-soluble vitamins, such as vitamin K, which

are carried by CM and their remnants (Havel et al. 1997), play an important role for osteoblastic function (Braam et al. 2003; Bolton-Smith et al. 2007). Vitamin K is essential for the γ-carboxylation of Gla-containing bone proteins, such as osteocalcin, and a suboptimal vitamin K status has been linked to osteoporosis (Newman et al. 2002). Analogously, ApoE null mice display a high bone mass phenotype that is caused by an increased bone formation rate, whereas bone resorption is not affected. The absence of ApoE in mice leads to a decreased uptake of triglyceride-rich lipoproteins and vitamin K by osteoblasts, resulting in elevated levels of undercarboxylated osteocalcin in serum (Schilling et al. 2005). According to this hypothesis, more bone was expected for low receptor affinity ApoE2 knockin mice in comparison to ApoE3 and ApoE4 animals. Surprisingly, this project clearly demonstrates an opposing effect for these mice with a significantly reduced bone formation rate, indicating the involvement of an additional crucial pathway that is influenced by ApoE2 and causes the low bone phenotype. Personal communication with Dr. Andreas Niemeier revealed an inhibition of the Wnt/β-catenin-signaling pathway by ApoE. Thus, ApoE deficiency results in a release of inhibition and, consequently, stimulated Wnt-signling. Whether the Wnt/β-catenin-signaling pathway is altered by respective ApoE isoforms and how this mechanism is modulated, remains to be elucidated. Mice harboring either gain-of-function or loss-of-function mutations in β-catenin in differentiated osteoblasts develop a high bone mass and a low bone mass phenotype, respectively. These phenotypes were primarily caused by altered bone resorption through the expression of OPG by osteoblasts (Glass et al. 2006). In addition, the Wnt/β-catenin-signaling pathway blocks osteoclastogenesis by increasing OPG/RANKL ratio. Both, significantly increased urinary DPD and decreased OPG/RANKL could be observed in ApoE2

mice compared to ApoE3 and Apo4 animals supporting the hypothesis of a possible alteration of the Wnt/β-catenin-signaling pathway by respective ApoE isoforms.

Interestingly, ApoE4 has been reported to be associated with reduced BMD and increased fracture risk compared the ApoE isoform (Shiraki et al. 1997; Kohlmeier et al. 1998; Dick et al. 2002; Lee et al. 2005) whereas other studies could not confirm this association (Heikkinen et al. 2000; Stulc et al. 2000; Sennels et al. 2003). We could show that ApoE4 mice display significantly reduced serum OCN and ALP levels, biomechanical stability, femoral cortical bone, and a clear non-significant trend in decreased femoral trabecular bone compared to ApoE3 animals. Although, compared to ApoE3 animals, ApoE4 mice did not reveal any altered BV/TV of trabecular bone in lumbar vertebrae, indicating site-specific effects in these mice, these findings may participate to clarify the controversial discussion about the ApoE4 isoform on fracture risk.

4.2.1 Part 1 - conclusions

In conclusion we demonstrate that ApoE polymorphisms have different effects on bone metabolism. This was expected since ApoE knockout mice display a high bone phenotype and several studies associate ApoE4 with lower BMD and increased fracture risk. The finding of decreased trabecular bone volume per total volume in femoral bone and lumbar spine in ApoE2 mice in comparison to ApoE3/E4 animals was surprising, since the low receptor affinity of ApoE2 and subsequent lower vitamin K uptake was expected to result in more bone due to elevated levels of undercarboxylated OCN. Thus, other crucial pathways involved in bone metabolism, e. g. Wnt/β-catenin-signaling pathways (personal communication), must be more affected by the ApoE2 polymorphism.

4.2.2 Part 1 – outlook

The current study did not distinguish whether the triglyceride transport, and therefore the vitamin K uptake is altered by ApoE2. Further studies will address possible alteration of OCN γ-carboxylation and its impact on osteoblast activity in respective ApoE mice. One of the further crucial goals of this project is the verification of observed murine phenotype in humans. Thus my collaborator, Dr. Andreas Niemeier, was able to organize human serum samples from patients carrying homozygous ApoE2, ApoE3, and ApoE4 alleles, respectively. These serum and urinary samples will be used to measure above mentioned bone turnover markers in order to show similar bone turnover patterns in humans. In addition to serum and urinary analysis, respective patients will be scanned in a computer tomography to verify murine bone phenotype of respective ApoE isoforms in humans. Comparable findings in humans will emphasize the importance of ApoE polymorphisms in bone metabolism and establish human ApoE knockin mice as a powerful model to investigate possible pathways relevant in osterporosis. After proving comparable findings in humans, the ultimate goal for this project will be the investigation of the mechanism that is altered by ApoE2 polymorphism and causes the low bone phenotype. A potential candidate is the Wnt/β-catenin-signaling pathway (personal communication), which is crucial in bone metabolism. Primary bone cell lines will be used to study this pathway for respective ApoE isoforms.

5. References

Aubin, J. E. (2001). *Regulation of osteoblast formation and function*. Rev Endocr Metab Disord 2, 81-94.

Baron, R. and Rawadi, G. (2007). *Targeting the Wnt/beta-catenin pathway to regulate bone formation in the adult skeleton*. Endocrinology 148, 2635-43.

Beisiegel, U., Weber, W. and Bengtsson-Olivecrona, G. (1991). *Lipoprotein lipase enhances the binding of chylomicrons to low density lipoprotein receptor-related protein*. Proc Natl Acad Sci USA 88, 8342-6.

Bellosta, S., Mahley, R. W., Sanan, D. A., Murata, J., Newland, D. L., Taylor, J. M. and Pitas, R. E. (1995). *Macrophage-specific expression of human apolipoprotein E reduces atherosclerosis in hypercholesterolemic apolipoprotein E-null mice*. J Clin Invest 96, 2170-9.

Bolton-Smith, C., McMurdo, M. E., Paterson, C. R., Mole, P. A., Harvey, J. M., Fenton, S. T., Prynne, C. J., Mishra, G. D. and Shearer, M. J. (2007). *Two-year randomized controlled trial of vitamin K1 (phylloquinone) and vitamin D3 plus calcium on the bone health of older women*. J Bone Miner Res 22, 509-19.

Boucher, P., Liu, P., Gotthardt, M., Hiesberger, T., Anderson, R. G. and Herz, J. (2002). *Platelet-derived growth factor mediates tyrosine phosphorylation of the cytoplasmic domain of the low density lipoprotein receptor-related protein in caveolae*. J Biol Chem 277, 15507-15513.

Boucher, P., Gotthardt, M., Li, W. P., Anderson, R. G. and Herz, J. (2003). *LRP: role in vascular wall integrity and protection from atherosclerosis*. Science 300, 329-332.

Boucher, P., Li, W. P., Matz, R. L., Takayama, Y., Auwerx, J., Anderson, R. G. and Herz, J. (2007). *LRP1 functions as an atheroprotective integrator of TGFbeta and PDFG signals in the vascular wall: implications for Marfan syndrome*. PLoS One 2, e448.

Boyle, W. J., Simonet, W. S. and Lacey, D. L. (2003). *Osteoclast differentiation and activation*. Nature 423, 337-42.

Braam, L. A., Knapen, M. H., Geusens, P., Brouns, F., Hamulyak, K., Gerichhausen, M. J. and Vermeer, C. (2003). *Vitamin K1 supplementation retards bone loss in postmenopausal women between 50 and 60 years of age*. Calcif Tissue Int 73, 21-6.

Bu, G. (2009). *Apolipoprotein E and its receptors in Alzheimer's disease: pathways, pathogenesis and therapy*. Nat Rev Neurosci 10, 333-44.

Cam, J. A., Zerbinatti, C. V., Li, Y. and Bu, G. (2005). *Rapid endocytosis of the low density lipoprotein receptor-related protein modulates cell surface distribution and processing of the beta-amyloid precursor protein*. J Biol Chem 280, 15464-70.

Capdevila, J. and Izpisua Belmonte, J. C. (2001). *Patterning mechanisms controlling vertebrate limb development*. Annu Rev Cell Dev Biol 17, 87-132.

Chen, W. J., Goldstein, J. L. and Brown, M. S. (1990). *NPXY, a sequence often found in cytoplasmic tails, is required for coated pit-mediated internalization of the low density lipoprotein receptor*. J Biol Chem 265, 3116-23.

Clarke, B. (2008). *Normal bone anatomy and physiology*. Clin J Am Soc Nephrol 3 Suppl 3, S131-9.

Clevers, H. (2006). *Wnt/beta-catenin signaling in development and disease*. Cell 127, 469-80.

Clevers, H. and van de Wetering, M. (1997). *TCF/LEF factor earn their wings*. Trends Genet 13, 485-9.

Cohen, M. M., Jr. (2006). *The new bone biology: pathologic, molecular, and clinical correlates*. Am J Med Genet A 140, 2646-706.

Corder, E. H., Saunders, A. M., Strittmatter, W. J., Schmechel, D. E., Gaskell, P. C., Small, G. W., Roses, A. D., Haines, J. L. and Pericak-Vance, M. A. (1993). *Gene dose of apolipoprotein E type 4 allele and the risk of Alzheimer's disease in late onset families*. Science 261, 921-3.

Curtiss, L.K., Boisvert, W. A. (2000). *Apolipoprotein E and atherosclerosis*. Curr Opin Lipidol 3, 243-51.

Davignon, J., Gregg, R. E. and Sing, C. F. (1988). *Apolipoprotein E polymorphism and atherosclerosis*. Arteriosclerosis 8, 1-21.

Deal, C. (2009). *Potential new drug targets for osteoporosis*. Nat Clin Pract Rheumatol 5, 20-7.

Deane, R., Wu, Z., Sagare, A., Davis, J., Du Yan, S., Hamm, K., Xu, F., Parisi, M., LaRue, B., Hu, H. W., Spijkers, P., Guo, H., Song, X., Lenting, P. J., Van Nostrand, W. E. and Zlokovic, B. V. (2004). *LRP/amyloid beta-peptide interaction mediates differential brain efflux of Abeta isoforms*. Neuron 43, 333-44.

Deng, Z. L., Sharff, K. A., Tang, N., Song, W. X., and He, T. C. (2008). *Regulation of osteogenic differentiation during skeletal development*. Front Biosci 13, 2001-21.

Dick, I. M., Devine, A., Marangou, A., Dhaliwal, S. S., Laws, S., Martins, R. N. and Prince, R. L. (2002). *Apolipoprotein E4 is associated with reduced calcaneal quantitative ultrasound measurements and bone mineral density in elderly women*. Bone 31, 497-502.

Dietrich, M. F., van der Weyden, L., Prosser, H. M., Bradley, A., Herz, J. and Adams, D. J. *Ectodomains of the LDL receptor-related proteins LRP1b and LRP4 have anchorage independent functions in vivo*. PLoS One 5, e9960.

Ding, L., Getz, G., Wheeler, D. A. and Wilson, R. K. (2008). *Somatic mutations affect key pathways in lung adenocarcinoma*. Nature 455, 1069-75.

Dong, L. M., Parkin, S., Trakhanov, S. D., Rupp, B., Simmons, T., Arnold, K. S., Newhouse, Y. M., Innerarity, T. L. and Weisgraber, K. H. (1996). *Novel mechanism for defective receptor binding of apolipoprotein E2 in type III hyperlipoproteinemia*. Nat Struct Biol 3, 718-22.

Drogemuller, C., Leeb, T., Harlizius, B., Tammen, I., Distl, O., Holtershinken, M., Gentile, A., Duchesne, A. and Eggen, A. (2007). *Congenital syndactyly in cattle: four novel mutations in the low density lipoprotein receptor-related protein 4 gene (LRP4)*. BMC Genet 8, 5.

Duchesne, A., Gautier, M., Chadi, S., Grohs, C., Floriot, S., Gallard, Y., Caste, G., Ducos, A. and Eggen, A. (2006). *Identification of a doublet missense substitution in the bovine LRP4 gene as a candidate causal mutation for syndactyly in Holstein cattle*. Genomics 88, 610-21.

Ducy, P., Desbois, C., Boyce, B., Pinero, G., Story, B., Dunstan, C., Smith, E., Bonadio, J., Goldstein, S., Gundberg, C. et al. (1996). *Increased bone formation in osteocalcin-deficient mice*. Nature 382, 448-52.

Eichner, J. E., Dunn, S. T., Perveen, G., Thompson, D. M., Stewart, K. E. and Stroehla, B. C. (2002). *Apolipoprotein E polymorphism and cardiovascular disease: a HuGE review*. Am J Epidemiol 155, 487-95.

Garnero, P. and Delmas, P. D. (1996). *New developments in biochemical markers for osteoporosis*. Calcif Tissue Int 59 Suppl 1, S2-9.

Ghiselli, G., Schaefer, E. J., Gascon, P. and Breser, H. B., Jr. (1981). *Type III hyperlipoproteinemia associated with apolipoprotein E deficiency*. Science 214, 1239-41.

Glass, D. A. and Karsenty, G. (2006). *Canonical Wnt signaling in osteoblasts is required for osteoclast differentiation*. Ann N Y Acad Sci 1068, 117-30.

Goldstein, J. L. and Brown, M. S. (2001). *Molecular medicine. The cholesterol quartet*. Science 292, 1310-2.

Gong, Y., Slee, R. B., Fukai, N., Rawadi, G., Roman-Roman, S., Reginato, A. M., Wang, H., Cundy, T., Glorieux, F. H., Lev, D. et al. (2001). *LDL receptor-related protein 5 (LRP5) affects bone accrual and eye development*. Cell 107, 513-23.

Gotthardt, M., Trommsdorff, M., Nevitt, M. F., Shelton, J., Richardson, J. A., Stockinger, W., Nimpf, J. and Herz, J. (2000). *Interactions of the low density lipoprotein receptor gene family with cytosolic adaptor and scaffold proteins suggest diverse biological functions in cellular communication and signal transduction*. J Biol Chem 275, 25616-24.

Grotewold, L. and Ruther, U. (2002). *The Wnt antagonist Dickkopf-1 is regulated by Bmp signaling and c-Jun and modulates programmed cell death*. EMBO J 21, 966-75.

Hagberg, J. M., Wilund, K. R. and Ferrell, R. E. (2000). *APO E gene and gene-environment effects on plasma lipoprotein-lipid levels*. Physiol Genomics 4, 101-108.

Hatters, D. M., Peters-Libeu, C. A. and Weisgraber, K. H. (2006). *Apolipoprotein E structure: insights into function*. Trends Biochem Sci 8, 445-54.

Havel, R. J. (1997). *Postprandial lipid metabolism: an overview*. Proc Nutr Soc 56, 659-66.

He, X. C., Zhang, J., Tong, W. G., Tawfik, O., Ross, J., Scoville, D. H., Tian, Q., Zeng, X., He, X., Wiedemann, L. M., Mishina, Y. and Li, L. (2004). *BMP signaling inhibits intestinal stem cell self-renewal through suppression of Wnt-beta-catenin signaling.* Nat Genet 36, 1117-21.

Heikkinen, A. M., Kroger, H., Niskanen, L., Komulainen, M. H., Ryynanen, M., Parviainen, M. T., Tuppurainen, M. T., Honkanen, R. and Saarikoski, S. (2000).

Does apolipoprotein E genotype relate to BMD and bone markers in postmenopausal women? Maturitas 34, 33-41.

Herz, J. and Bock, H. H. (2002). *Lipoprotein receptors in the nervous system*. Annu Rev Biochem 71, 405-34.

Herz, J. and Chen, Y. (2006). *Reelin, lipoprotein receptors and synaptic plasticity*. Nat Rev Neuroscience 7, 850-9.

Herz, J. (2009). *Apolipoprotein E receptors in the nervous system*. Curr Opin Lipidol 20, 190-6.

Herz, J., Chen, Y., Masiulis, I. and Zhou, L. (2009). *Expanding functions of lipoprotein receptors*. J Lipid Res 50 Suppl, S287-92.

Heymann, D. and Rousselle, A. V. (2000). *gp130 Cytokine family and bone cells*. Cytokine 12, 1455-68.

Hobbs, H. H., Russel, D. W., Brown, M. S. and Goldstein, J. L. (1990). *The LDL receptor locus in familial hypercholesterolemia: mutational analysis of a membrane protein*. Annu Rev Genet 24, 133-77.

Holmen, S. L., Giambernardi, T. A., Zylstra, C. R. and Williams, B. O. (2004). *Decreased BMD and limb deformities in mice carrying mutations in both Lrp5 and Lrp6.* J Bone Miner Res 19, 2033-40.

Johnson, E. B., Hammer, R. E. and Herz, J. (2005). *Abnormal development of the apical ectodermal ridge and polysyndactyly in Megf7-deficient mice*. Hum Mol Genet 14, 3523-38.

Karner, C. M., Dietrich, M. F., Johnson, E. B., Kappesser, N., Tennert, C., Percin, F., Wollnik, B., Carroll, T. J. and Herz, J. *Lrp4 regulates initiation of ureteric budding and is crucial for kidney formation--a mouse model for Cenani-Lenz syndrome*. PLoS One 5, e10418.

Kearns, A. E., Khosla, S. and Kostenuik, P. J. (2008). *Receptor activator of nuclear factor kappaB ligand and osteoprotegerin regulation of bone remodeling in health and disease*. Endocr Rev 29, 155-92.

Kim, N., Stiegler, A. L., Cameron, T. O., Hallock, P. T., Gomez, A. M., Huang, J. H., Hubbard, S. R., Dustin, M. L. and Burden, S. J. (2008). *Lrp4 is a receptor for Agrin and forms a complex with MuSK*. Cell 135, 334-42.

Knouff, C., Hinsdale, M. E., Mezdour, H., Altenburg, M. K., Watanabe, M., Quarfordt, S. H., Sullivan, P. M. and Maeda, N. (1999). *Apo E structure determines VLDL clearance and atherosclerosis risk in mice*. J Clin Invest 103, 1579-86.

Kobayashi, T., Lyons, K. M., McMahon, A. P., Kronenberg, H. M. (2005). *BMP signaling stimulates cellular differentiation at multiple steps during cartilage development*. Proc Natl Acad Sci U S A 102, 18023-7.

Kohlmeier, M., Saupe, J., Schaefer, K. and Asmus, G. (1998). *Bone fracture history and prospective bone fracture risk of hemodialysis patients are related to apolipoprotein E genotype*. Calcif Tissue Int 62, 278-81.

Krishnan, V., Bryant, H. U. and Macdougald, O. A. (2006). *Regulation of bone mass by Wnt signaling*. J Clin Invest 116,1202-9.

Lacey, D. L., Timms, E., Tan, H. L., Kelley, M. J. and Boyle W, J. (1998). *Osteoprotegerin ligand is a cytokine that regulates osteoclast differentiation and activation*. Cell 93, 165-76.

Langbein, S., Szakacs O., Wilhelm M., Sukosd F., Weber S., et al. (2002). *Alteration of the LRP1B gene region is associated with high grade of urothelial cancer*. Lab Invest *82*, 639-43.

Lee, S. I., Lee, S. Y. and Yoo, W. H. (2005). *Association of apolipoprotein E polymorphism with bone mineral density in postmenopausal women with rheumatoid arthritis*. Rheumatology (Oxford) 44, 1067-8.

Li, W. H., Tanimura, M., Luo, C. C., Datta, S. and Chan, L. (1988). *The apolipoprotein multigene family: biosynthesis, structure, structure-function relationships, and evolution*. J Lipid Res 3, 245-71.

Li, X., Ominsky, M. S., Niu, Q. T., Sun, N., Daugherty, B., D'Agostin, D., Kurahara, C., Gao, Y., Cao, J., Gong, J. et al. (2008). *Targeted deletion of the sclerostin gene in mice results in increased bone formation and bone strength*. J Bone Miner Res 23, 860-9.

Li, Y., Marzolo, M. P., van Kerkhof, P., Strous, G. J. and Bu, G. (2000). *The YXXL motif, but not the two NPXY motifs, serves as the dominant endocytosis signal for low density lipoprotein receptor-related protein*. J Biol Chem 275, 17187-17194

Li, Y., Pawlik, B., Elcioglu, N., Aglan, M., Kayserili, H., Yigit, G., Percin, F., Goodman, F., Nurnberg, G., Cenani, A. et al. (2010). *LRP4 mutations alter Wnt/beta-catenin signaling and cause limb and kidney malformations in Cenani-Lenz syndrome*. Am J Hum Genet 86, 696-706.

Lin, J. T. and Lane, J. M. (2004). *Osteoporosis: a review*. Clin Orthop Relat Res, 126-34.

Little, R. D., Carulli, J. P., Del Mastro, R. G., Dupuis, J., Osborne, M., Folz, C., Manning, S. P., Swain, P. M., Zhao, S. C., Eustace, B. et al. (2002). *A mutation in the LDL receptor-related protein 5 gene results in the autosomal dominant high-bone-mass trait*. Am J Hum Genet 70, 11-9.

Liu, C. X., Musco, S., Lisitsina, N. M., Yaklichkin, S. Y. and Lisitsyn; N. A. (2000). *Genomice organization of a new candidate tumor suppressor gene, LRP1B*. Genomics 69, 271-74.

Liu, F., Kohlmeier, S. and Wang, C. Y. (2008). *Wnt-signaling and skeletal development*. Cell Signal 20, 999-1009.

Logan, C. Y. and Nusse, R. (2004). *The Wnt-signaling pathway in development and disease*. Annu Rev Cell Dev Biol 20, 781-810.

Loots, G. G., Kneissel, M., Keller, H., Baptist, M., Chang, J., Collette, N. M., Ovcharenko, D., Plajzer-Frick, I. and Rubin, E. M. (2005). *Genomic deletion of a long-range bone enhancer misregulates sclerostin in Van Buchem disease*. Genome Res 15, 928-35.

MacDonald, B. T., Adamska, M. and Meisler, M. H. (2004). *Hypomorphic expression of Dkk1 in the doubleridge mouse: dose dependence and compensatory interactions with Lrp6*. Development 131, 2543-52.

Mahley, R. W. (1988). *Apolipoprotein E: cholesterol transport protein with expanding role in cell biology*. Science 240, 622-30.

Mahley, R. W. and Ji, Z. S. (1999). *Remnant lipoprotein metabolism: key pathways involving cell-surface heparan sulfate proteoglycans and apolipoprotein E*. J Lipid Res 40, 1-16.

Mahley, R. W. and Rall, S. C. Jr. (2000). *Apolipoprotein E: far more than a lipid transport protein*. Annu Rev Genomics Hum Genet 1, 507-37.

Mao, B., Wu, W., Li, Y., Hoppe, D., Stannek, P., Glinka, A. and Niehrs, C. (2001). *LDL-receptor-related protein 6 is a receptor for Dickkopf proteins*. Nature 411, 321-5.

Martins, R. N., Clarnette, R., Fisher, C., Broe, G. A., Brooks, W. S., Montgomery, P. and Gandy, S. E. (1995). *ApoE genotypes in Australia: roles in early and late onset Alzheimer's disease and Down's syndrome*. Neuroreport 6, 1513-6.

May, P. and Herz, J. (2003). *LDL receptor-related proteins in neurodevelopment*. Traffic 4, 291-301.

May, P., Herz, J. and Bock, H. H. (2005). *Molecular mechanisms of lipoprotein receptor signalling*. Cell Mol Life Sci 62, 2325-38.

Moon, R. T., Kohn, A. D., De Ferrari, G. V. and Kaykas, A. (2004). *WNT and beta-catenin signalling: diseases and therapies*. Nat Rev Genet 5, 691-701.

Morvan, F., Boulukos, K., Clement-Lacroix, P., Roman Roman, S., Suc-Royer, I., Vayssiere, B., Ammann, P., Martin, P., Pinho, S., Pognonec, P. et al. (2006). *Deletion of a single allele of the Dkk1 gene leads to an increase in bone formation and bone mass*. J Bone Miner Res 21, 934-45.

Mukhopadhyay, M., Shtrom, S., Rodriguez-Esteban, C., Chen, L., Tsukui, T., Gomer, L., Dorward, D. W., Glinka, A., Grinberg, A., Huang, S. P. et al. (2001). *Dickkopf1 is required for embryonic head induction and limb morphogenesis in the mouse*. Dev Cell 1, 423-34.

Nakagawa, T., Pimkhaokham A., Suzuki E., Omura K., Inazawa J., et al. (2006). *Genetic or epigenetic silencing of low density lipoprotein receptor-related protein 1B expression in oral squamous cell carcinoma*. Cancer Sci *97*, 1070-4.

Nakashima, K. and de Crombrugghe, B. (2003). *Transcriptional mechanisms in osteoblast differentiation and bone formation*. Trends Genet 19, 458-66.

Nakayama, M., Nakajima, D., Nagase, T., Nomura, N., Seki, N. and Ohara, O. (1998). *Identification of high-molecular-weight proteins with multiple EGF-like motifs by motif-trap screenin*g. Genomics 51, 27-34.

Newman, P., Bonello, F., Wierzbicki, A. S., Lumb, P., Savidge, G. F. and Shearer, M. J. (2002). *The uptake of lipoprotein-borne phylloquinone (vitamin K1) by osteoblasts and osteoblast-like cells: role of heparan sulfate proteoglycans and apolipoprotein E*. J Bone Miner Res 17, 426-33.

Niemeier, A., Kassem, M., Toedter, K., Wendt, D., Ruether, W., Beisiegel, U. and Heeren, J. (2005). *Expression of LRP1 by human osteoblasts: a mechanism for the delivery of lipoproteins and vitamin K1 to bone*. J Bone Miner Res 20, 283-93.

Niemeier, A., Niedzielska, D., Secer, R., Schilling, A., Merkel, M., Enrich, C., Rensen, P. C. and Heeren, J. (2008). *Uptake of postprandial lipoproteins into bone in vivo: impact on osteoblast function*. Bone 43, 230-7.

Nykjaer, A., Dragun D., Walther D., Vorum H., Jacobsen C., et al. (1999). *An endocytic pathway essential for renal uptake and activation of the steroid 25-(OH) vitamin D3*. Cell *96*, 507-15

Nykjaer, A. and Willnow, T. E. (2002). *The low-density lipoprotein receptor gene family: a cellular Swiss army knife?* Trends Cell Biol 12, 273-80.

Ohazama, A., Johnson, E. B., Ota, M. S., Choi, H. Y., Porntaveetus, T., Oommen, S., Itoh, N., Eto, K., Gritli-Linde, A., Herz, J. et al. (2008). *Lrp4 modulates extracellular integration of cell signaling pathways in development*. PLoS One 3, e4092.

Perry, M. J., McDougall, K .E., Hou, S. C and Tobias J. H. (2008). *Impaired growth plate function in bmp-6 null mice*. Bone 42, 216-25.

Pinson, K. I., Brennan, J., Monkley, S., Avery, B. J. and Skarnes, W. C. (2000). *An LDL-receptor-related protein mediates Wnt signalling in mice*. Nature 407, 535-8.

Rahmatpanah, F.B., Carstens S., Guo J., Sjahputera O., Taylor K.H., et al. (2006). *Differential DNA methylation patterns of small B-cell lymphoma subclasses with different clinical behavior*. Leukemia *20*, 1855-62.

Richards, J. B., Kavvoura, F. K., Rivadeneira, F., Styrkarsdottir, U., Estrada, K., Halldorsson, B. V., Hsu, Y. H., Zillikens, M. C., Wilson, S. G., Mullin, B. H. et al. (2009). *Collaborative meta-analysis: associations of 150 candidate genes with osteoporosis and osteoporotic fracture*. Ann Intern Med 151, 528-37.

Rivadeneira, F., Styrkarsdottir, U., Estrada, K., Halldorsson, B. V., Hsu, Y. H., Richards, J. B., Zillikens, M. C., Kavvoura, F. K., Amin, N., Aulchenko, Y. S. et al.

(2009). *Twenty bone-mineral-density loci identified by large-scale meta-analysis of genome-wide association studies*. Nat Genet 41, 1199-206.

Rousselle, A. V. and Heymann, D. (2002). *Osteoclastic acidification pathways during bone resorption*. Bone 30, 533-40.

Roversi, G., Pfundt R., Moroni R.F., Magnani I., van Reijmersdal S., et al. (2006). *Identification of novel genomic markers related to progression to glioblastoma through genomic profiling of 25 primary glioma cell lines*. Oncogene *25*, 1571-83.

Schilling, A. F., Schinke, T., Münch, C., Gebauer, M., Niemeier, A., Priemel, M, Streichert, T., Rueger, J. M. and Amling, M. (2005). *Increased bone formation in mice lacking apolipoprotein E*. J Bone Miner Res 2,274-82.

Segrest, J. P., Garber, D. W., Brouillette, C. G., Harvey, S. C. and Anantharamaiah, G. M. (1994). *The amphipathic alpha helix: a multifunctional structural motif in plasma apolipoproteins*. Adv Protein Chem 45, 303-69.

Segrest, J. P., Jones, M. K., De Loof, H., Brouillette, C. G., Venkatachalapathi, Y. V. and Anantharamaiah, G. M. (1992). *The amphipathic helix in the exchangeable apolipoproteins: a review of secondary structure and functio*n. J Lipid Res 33, 141-66.

Selkoe, D. J. (2002). *Deciphering the genesis and fate of amyloid beta-protein yields novel therapies for Alzheimer disease*. J Clin Invest 110, 1375-81.

Sennels, H. P., Sand, J. C., Madsen, B., Lauritzen, J. B., Fenger, M. and Jorgensen, H. L. (2003). *Association between polymorphisms of apolipoprotein E, bone mineral density of the lower forearm, quantitative ultrasound of the calcaneus and osteoporotic fractures in postmenopausal women with hip or lower forearm fracture*. Scand J Clin Lab Invest 63, 247-58.

Shibata, M., Yamada, S., Kumar, S. R., Calero, M., Bading, J., Frangione, B., Holtzman, D. M., Miller, C. A., Strickland, D. K., Ghiso, J. and Zlokovic BV. (2000).

Clearance of Alzheimer's amyloid-ss (1-40) peptide from brain by LDL receptor-related protein-1 at the blood-brain barrier. J Clin Invest106,1489-99.

Shimano, H., Yamada, N., Katsuki, M., Shimada, M., Gotoda, T., Harada, K., Murase, T., Fukazawa, C., Takaku, F. and Yazaki, Y. (1992). *Overexpression of apolipoprotein E in transgenic mice: marked reduction in plasma lipoproteins except high density lipoprotein and resistance against diet-induced hypercholesterolemia*. Proc Natl Acad Sci U S A 89, 1750-4.

Shiraki, M., Shiraki, Y., Aoki, C., Hosoi, T., Inoue, S., Kaneki, M. and Ouchi, Y. (1997). *Association of bone mineral density with apolipoprotein E phenotype*. J Bone Miner Res 12, 1438-45.

Simon-Chazottes, D., Tutois, S., Kuehn, M., Evans, M., Bourgade, F., Cook, S., Davisson, M. T. and Guenet, J. L. (2006). *Mutations in the gene encoding the low-density lipoprotein receptor LRP4 cause abnormal limb development in the mouse*. Genomics 87, 673-7.

Simonet, W. S., Bucay, N., Lauer, S. J., Wirak, D. O., Stevens, M. E., Weisgraber, K. H., Pitas, R. E. and Taylor, J. M. (1990). *In the absence of a downstream element, the apolipoprotein E gene is expressed at high levels in kidneys of transgenic mice*. J Biol Chem 265, 10809-12.

Sipos, W., Pietschmann, P., Rauner, M., Kerschan-Schindl, K. and Patsch, J. (2009). *Pathophysiology of osteoporosis*. Wien Med Wochenschr 159, 230-4.

Sonoda, I., Imoto I., Inoue J., Shibata T., Shimada Y. (2004). *Frequent silencing of low density lipoprotein receptor-related protein 1B (LRP1B) expression by genetic and epigenetic mechanisms in esophageal squamous cell carcinoma*. Cancer Res *64*, 3741-7.

Spoelgen, R., Hammes, A., Anzenberger, U., Zechner, D., Andersen, O. M., Jerchow, B. and Willnow, T. E. (2005). *LRP2/megalin is required for patterning of the ventral telencephalon*. Development 132, 405-14.

Strittmatter, W. J., Saunders, A. M., Schmechel, D., Pericak-Vance, M., Enghild, J., Salvesen, G. S. and Roses, A. D. (1993). *Apolipoprotein E: high-avidity binding to beta-amyloid and increased frequency of type 4 allele in late-onset familial Alzheimer disease*. Proc Natl Acad Sci U S A 90, 1977-81.

Stulc, T., Ceska, R., Horinek, A. and Stepan, J. (2000). *Bone mineral density in patients with apolipoprotein E type 2/2 and 4/4 genotype*. Physiol Res 49, 435-9.

Sullivan, P. M., Mezdour, H., Aratani, Y., Knouff, C., Najib, J., Reddick, R. L., Quarfordt, S. H. and Maeda, N. (1997). *Targeted replacement of the mouse apolipoprotein E gene with the common human APOE3 allele enhances diet-induced hypercholesterolemia and atherosclerosis*. J Biol Chem 272, 17972-80.

Sullivan, P. M., Mezdour, H., Quarfordt, S. H. and Maeda, N. (1998). *Type III hyperlipoproteinemia and spontaneous atherosclerosis in mice resulting from gene replacement of mouse Apoe with human Apoe*2*. J Clin Invest 102, 130-5.

Taichman, R. S. (2005). *Blood and bone: two tissues whose fates are intertwined to create the hematopoietic stem-cell niche*. Blood 105, 2631-9.

Takayama, Y., May, P., Anderson, R. G. and Herz, J. (2005). *Low density lipoprotein receptor-related protein 1 (LRP1) controls endocytosis and c-CBL-mediated ubiquitination of the platelet-derived growth factor receptor beta (PDGFR beta)*. J Biol Chem 280, 18504-10.

Takayanagi, H., Kim, S., Matsuo, K., Suzuki, H., Suzuki, T., Sato, K., Yokochi, T., Oda, H., Nakamura, K., Ida, N., Wagner, E. F. and Taniguchi, T. (2002). *RANKL maintains bone homeostasis through c-Fos-dependent induction of interferon-beta*. Nature 416, 744-9.

Tamai, K., Semenov, M., Kato, Y., Spokony, R., Liu, C., Katsuyama, Y., Hess, F., Saint-Jeannet, J. P. and He, X. (2000). *LDL-receptor-related proteins in Wnt signal transduction*. Nature 407, 530-5.

Taylor, K.H., Pena-Hernandez K.E., Davis J.W., Arthur G.L., Duff D.J., et al. (2007). *Large-scale CpG methylation analysis identifies novel candidate genes and reveals methylation hotspots in acute lymphoblastic leukemia*. Cancer Res *67*, 2617-25.

Teitelbaum, S. L. (2000). *Bone resorption by osteoclasts*. Science 289, 1504-8.

Trommsdorff, M., Gotthardt, M., Hiesberger, T., Shelton, J., Stockinger, W., Nimpf, J., Hammer, R. E., Richardson, J. A. and Herz, J. (1999). *Reeler/Disabled-like disruption of neuronal migration in knockout mice lacking the VLDL receptor and ApoE receptor 2*. Cell 97, 689-701.

Tybulewicz, V. L., Crawford, C. E., Jackson, P. K., Bronson, R. T. and Mulligan, R. C. (1991). *Neonatal lethality and lymphopenia in mice with a homozygous disruption of the c-abl proto-oncogene*. Cell 65, 1153-63.

Vance, J. E. and Hayashi, H. (2010). *Formation and function of apolipoprotein E-containing lipoproteins in the nervous system*. Biochim Biophys Acta 1801, 806-18.

Watkins, B. A., Li, Y., Lippman, H. E. and Feng, S. (2003). *Modulatory effect of omega-3 polyunsaturated fatty acids on osteoblast function and bone metabolism*. Prostaglandins Leukot Essent Fatty Acids 68, 387-98.

Weatherbee, S. D., Anderson, K. V. and Niswander, L. A. (2006). *LDL-receptor-related protein 4 is crucial for formation of the neuromuscular junction*. Development 133, 4993-5000.

Weintraub, M. S., Eisenberg, S. and Breslow, J. L. (1987). *Dietary fat clearance in normal subjects is regulated by genetic variation in apolipoprotein E*. J Clin Invest 80, 1571-7.

Weisgraber, K. H., Innerarity, T. L. and Mahley, R. W. (1982). *Abnormal lipoprotein receptor-binding activity of the human E apoprotein due to cysteine-arginine interchange at a single site*. J Biol Chem 257, 2518-21.

Weisgraber, K. H., Rall, S. C., Jr. and Mahley, R. W. (1981). *Human E apoprotein heterogeneity. Cysteine-arginine interchanges in the amino acid sequence of the apo-E isoforms*. J Biol Chem 256, 9077-83.

Winkler, D. G., Sutherland, M. K., Geoghegan, J. C., Yu, C., Hayes, T., Skonier, J. E., Shpektor, D., Jonas, M., Kovacevich, B. R., Staehling-Hampton, K. et al. (2003). *Osteocyte control of bone formation via sclerostin, a novel BMP antagonist*. EMBO J 22, 6267-76.

Yasuda, H., Shima, N., Nakagawa, N., Yamaguchi, K., Kinosaki, M., Mochizuki, S., Tomoyasu, A., Yano, K., Goto, M., Murakami, A. et al. (1998). *Osteoclast differentiation factor is a ligand for osteoprotegerin/osteoclastogenesis-inhibitory factor and is identical to TRANCE/RANKL*. Proc Natl Acad Sci U S A 95, 3597-602.

Zhang, B., Luo, S., Wang, Q., Suzuki, T., Xiong, W. C. and Mei, L. (2008). *LRP4 serves as a coreceptor of agrin*. Neuron 60, 285-97.

Zhang, S. H., Reddick, R. L., Piedrahita, J. A. and Maeda, N. (1992). *Spontaneous hypercholesterolemia and arterial lesions in mice lacking apolipoprotein E*. Science 258, 468-71.

Zhou, L., Takayama, Y., Boucher, P. Tallquist, M. D. And Herz, J. (2009). *LRP1 regulates architecture of the vascular wall by controlling PDGFRbeta-dependent phosphatidylinositol 3-kinase activation*. PLoS One 4, e6922.